National Aeronautics and Space Administration



Venus Intrepid Tessera Lander

Mission Concept Study Report to the NRC Decadal Survey Inner Planets Panel

Science Co-Champions: Dr. Martha S. Gilmore, Wesleyan University
Dr. Lori S. Glaze, NASA's Goddard Space Flight Center
Study Points of Contact: Charles L. Baker, NASA's Goddard Space Flight Center
George J. Tahu, NASA Headquarters

NASA-GSFC • NASA-ARC March 19, 2010

Venus Intrepid Tessera Lander

Final Report

Presented to the Planetary Decadal Survey Steering Committee and Inner Planets Panel

6 April 2010

Martha S. Gilmore
Science Co-Champion
Wesleyan University

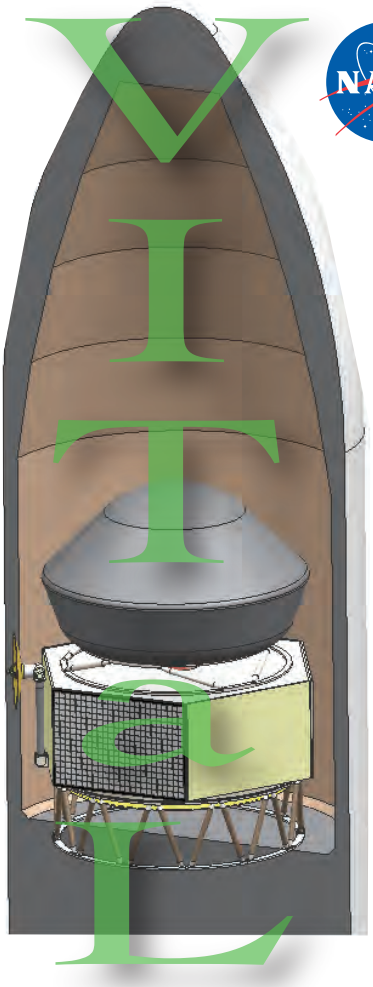
Lori S. Glaze
Science Co-Champion
NASA Goddard Space Flight Center

Michael L. Adams
Study Lead
NASA Goddard Space Flight Center

Charles L. Baker
Study Systems Lead
NASA Goddard Space Flight Center

Gabriel Karpati
Decadal Studies System Lead
NASA Goddard Space Flight Center

Michael J. Amato
Planetary and Lunar Business Lead
NASA Goddard Space Flight Center



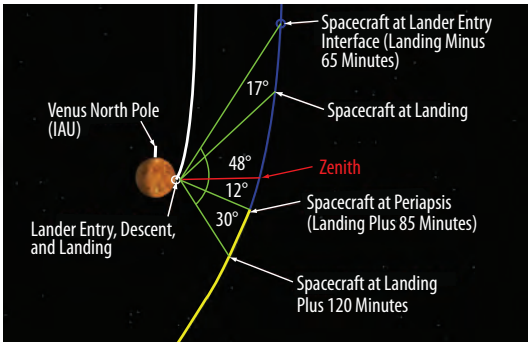
Venus Intrepid Tessera Lander

fact sheet

Mission Concept Study Report to the NRC Decadal Survey
Inner Planets Panel • March 15, 2010
Concept Maturity Level: 4 • Cost Range: Low End Flagship
GSFC • ARC

Nominal Mission:

- Atlas V 551 Launch Vehicle
- Type II trajectory
- Launch on 11/2/2021
- Venus fly-by 4/7/2022
- Descent/Landed science 7/29/2022

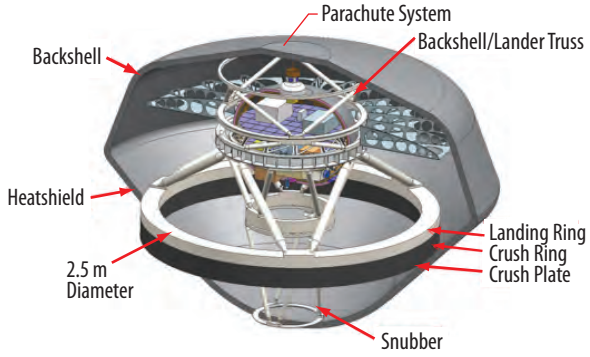


Note: At zenith the carrier S/C is directly overhead of the lander.

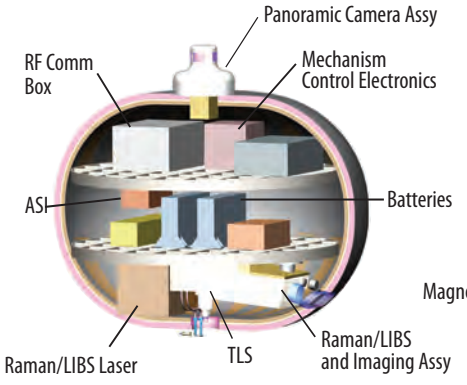
Mission Driving Science Objectives	Measurement	Instrument	Functional Requirement
Characterize chemistry and mineralogy of the surface.	Major, trace elements, mineralogy, NIR spectroscopy	Raman/LIBS; NIR (1.0 micron) descent imager below 1 km, Raman/LIBS context camera	Access to tessera terrain, > 25 *in situ* sample measurements, sample context images
Place constraints on the size and temporal extent of a possible ocean in Venus's past.	Measure D/H ratio in atmospheric water, mineralogy and major element chemistry of surface rocks.	NMS; TLS; Raman/LIBS	*In situ* sampling of the upper and lower (<16 km) atmosphere. Access to and measurement of tessera terrain.
Characterize the morphology and relative stratigraphy of surface units.	Visible and NIR observations of multiple surface units at cm to m scale spatial resolution.	NIR (1.0 micron) descent imager and surface panoramic camera with ~5 filters from 550-1000 nm.	Position of cameras to image the surface, while accommodating expected slopes, platform stability for clear images.

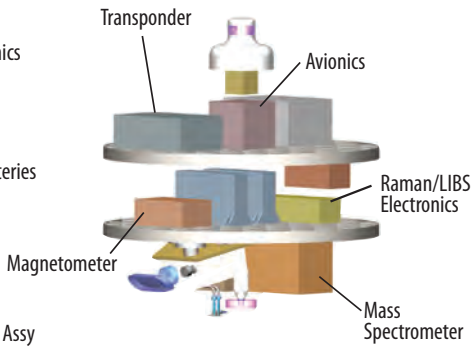
Lander Aeroshell (Cruise Configuration)

A low center of gravity Ring Lander in the Aeroshell

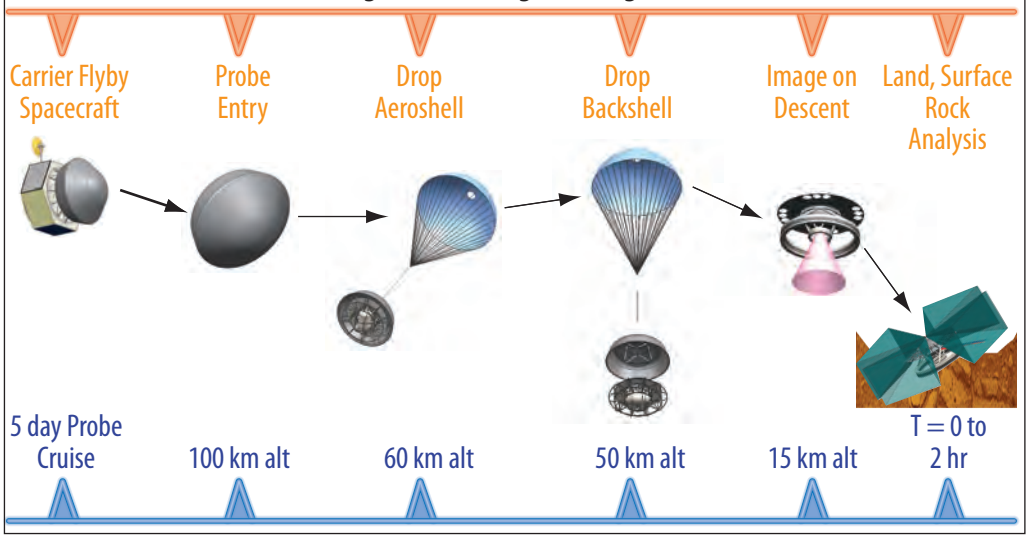


Pressure Vessel (Transparent View)

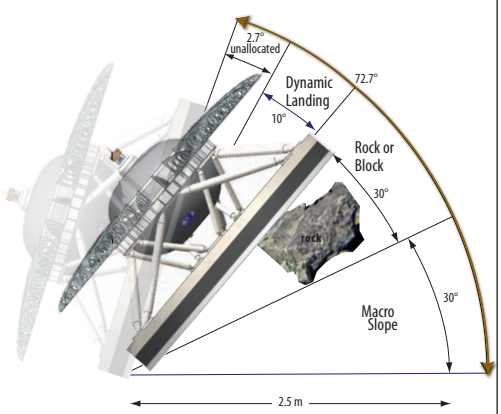




Probe timeline illustrates configuration changes throughout science mission duration.



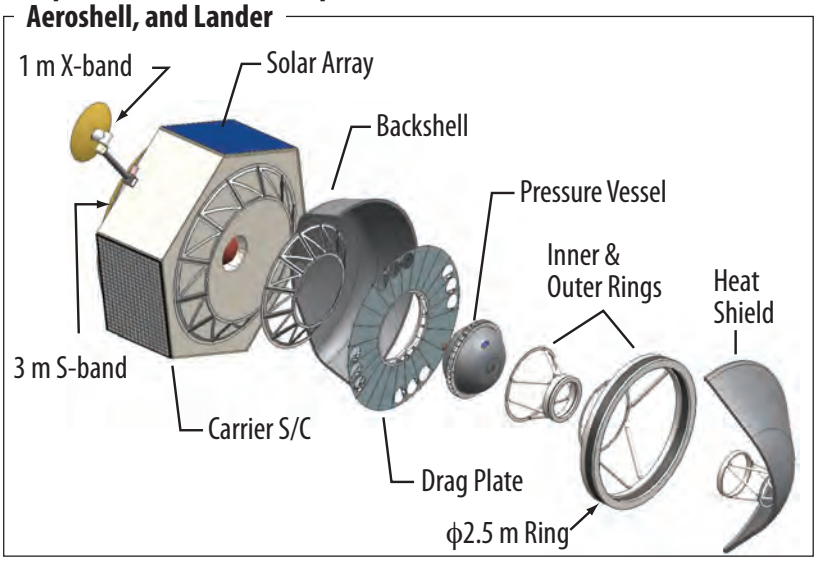
Ring design landing slope capability.



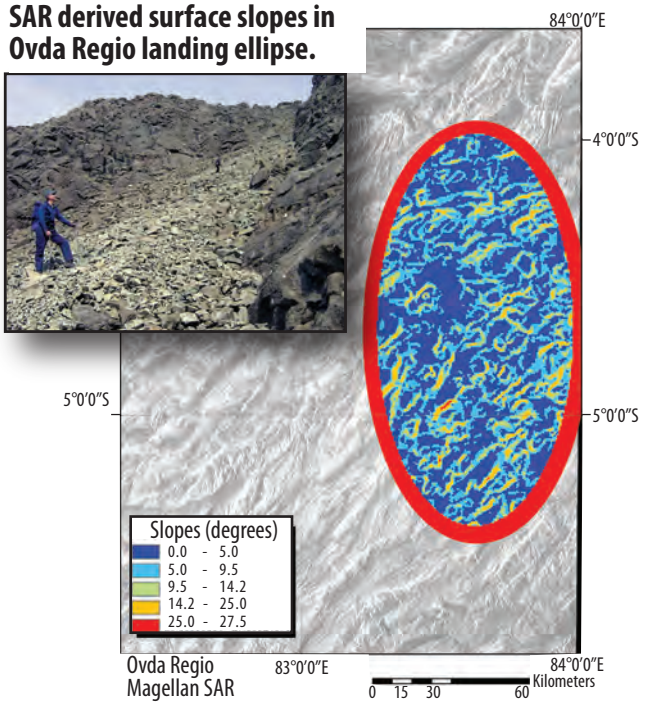
Venus Intrepid Tessera Lander

fact sheet

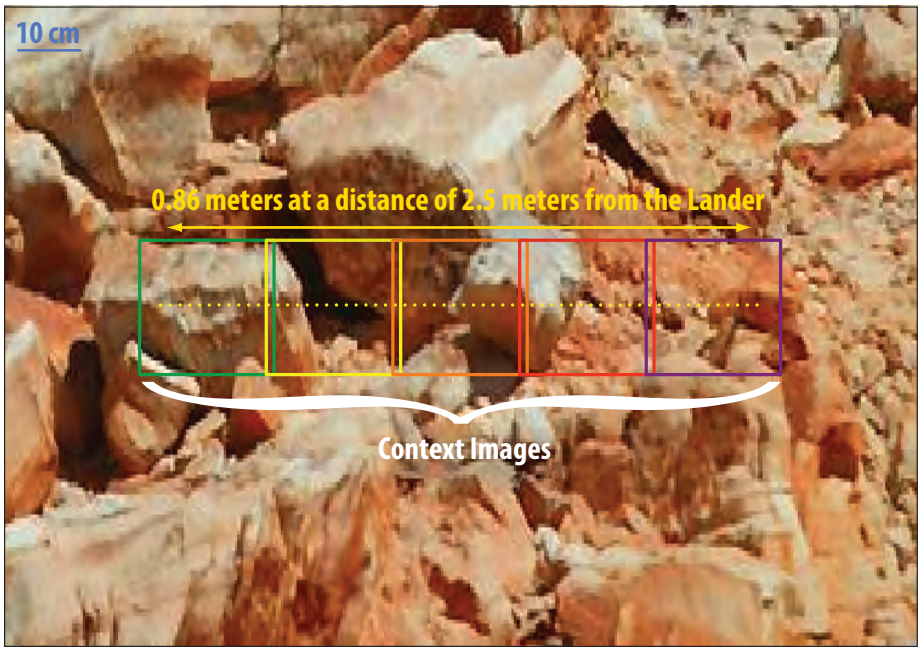
Exploded view of Carrier Spacecraft, Aeroshell, and Lander

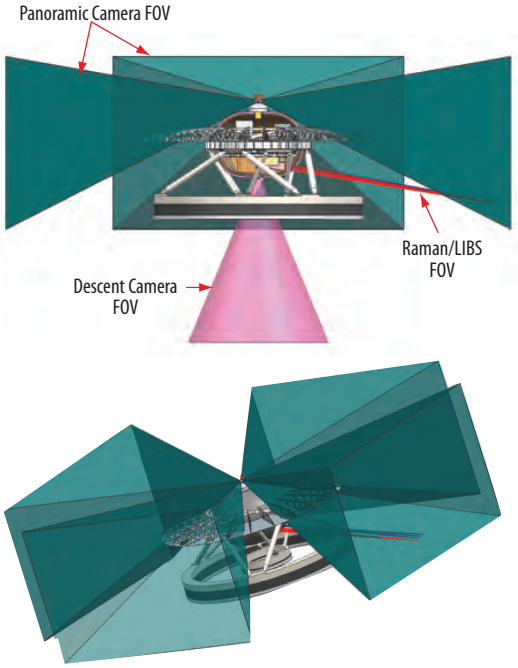


SAR derived surface slopes in Ovda Regio landing ellipse.

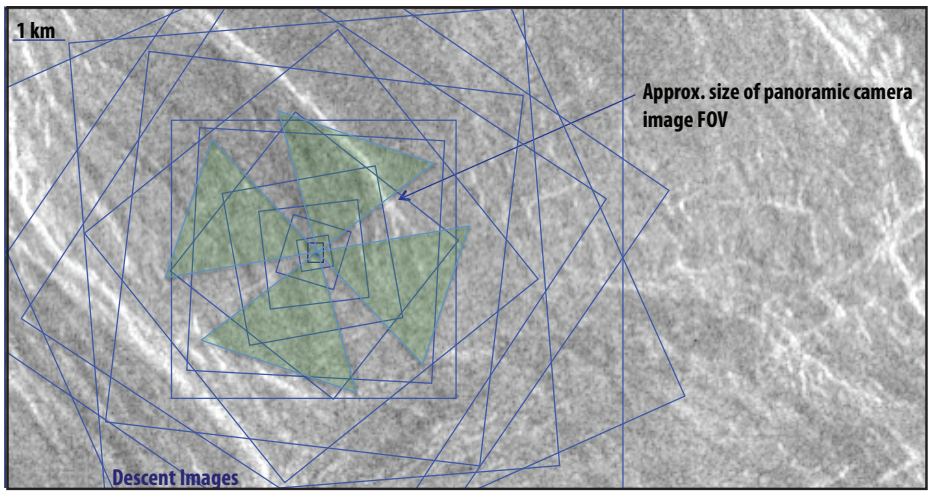


Raman/LIBS Survey Measurements and Context Images





Descent and Panoramic Imagery



Mass Breakdown

Component	CBE [kg]	Allow [%]	Max Mass [kg]
Lander	1051	30%	1366
Lander Science Payload & Accum.	48	30%	63
Lander Subsystems	1002	30%	1303
Mechanical/Structure	283	30%	368
Landing System	603	30%	784
Thermal	67	30%	87
Power	12	30%	16
Avionics	28	30%	36
RF Comm	9	30%	12
Aeroshell	1051	30%	1379
Spacecraft	846	30%	1100
Satellite *(S/C + Probe)* Dry Mass	2948	30%	3845
Satellite Wet Mass	3299	30%	4200
LV Throw Mass available to lift Wet			5141

TABLE OF CONTENTS

Executive Summary 1

1.0 Scientific Objectives 2
1.1 Scientific Questions and Objectives 2
1.2 Science Traceability 2
1.3 Study Objectives 4

2.0 High-Level Mission Concept 4
2.1 Overview 4
2.2 Concept Maturity Level 5

3.0 Technical Overview 6
3.1 Instrument Payload Implementation 6
3.2 Flight System 8
3.2.1 Concept of Operations and Mission Design 8
3.2.2 Carrier Spacecraft 11
3.2.3 Entry and Descent Element 11
3.2.4 Lander 12
3.2.4.1 Lander Structure 12
3.2.4.2 Lander Mechanical Static and Dynamic Analysis 14
3.2.4.3 Lander Mechanisms 15
3.2.4.4 Lander Thermal 16
3.2.4.5 Lander Optics 16
3.2.4.6 Lander Avionics 18
3.2.4.7 Lander Communications 19
3.2.4.8 Lander Power 19
3.2.4.9 Lander Mass and Data Rate 19
3.3 Ground Systems 20
3.4 Key Trades 22
3.4.1 Lander Design Trade 22
3.4.2 Crushable Material Trade 23
3.4.3 Hazard Avoidance System Trade 23
3.4.4 Communications with Steeper Slopes 24
3.4.5 Other Trades 24
3.5 Risk List 25
3.6 Technology Maturity 25

4.0 Development Schedule and Schedule Constraints 26
4.1 High-Level Mission Schedule 26
4.2 Technology Development Plan 26

5.0 Mission Life-Cycle Cost 27
5.1 Costing Methodology and Basis of Estimate 27
5.2 Cost Estimate 27

6.0 Conclusions 27

7.0 Open Topics 28

Acknowledgements 29

Appendix A – ADL Process 30
Appendix B – Alternative Landing Ellipses 31
Appendix C – Drag Plate Size Versus Velocity 32
Appendix D – Aeroshell Details 33
Appendix E – Context Imager 34
Appendix F - Acronyms List 35
Appendix G - References 36

Executive Summary

The National Research Council's 2010 Planetary Decadal Survey Inner Planets Panel commissioned the Goddard Space Flight Center's (GSFC) Architecture Design Lab (ADL) to do an enhanced rapid mission architecture study, conducted under NASA Headquarters leadership. The charge was to conceive a Venus mission architecture capable of safe landing in one of the mountainous tessera regions of the planet on a budget comparable to New Frontiers. Using the ADL's five step process (see Appendix), the study accomplished a systematic exploration, down-selection, and optimization of the best architecture concepts for the Venus Intrepid Tessera Lander (VITaL).

Based on analyses of the landing dynamics, mechanical, thermal, power, optics, avionics, and communication designs for VITaL, the study team can state with confidence that a robust lander capable of landing safely in the tessera terrain conducting surface science, and transmitting all data back to the telecom relay spacecraft (S/C) is technically feasible. The cost estimate for the nominal baseline VITaL implementation ($740M to 1.1B FY15, not including launch vehicle) is from the high end of the New Frontiers range to the low end of the Flagship range. Descopes that focus the mission on the three highest priority science objectives result in a mission that has a higher probability of fitting within a New Frontiers budget. The lander was designed with high TRL components to minimize both cost and risk. Following completion of this study, the VITaL Concept Maturity Level (CML) is raised from 2 to 4.

The VITaL mission concept provides key surface chemistry and mineralogy measurements in a tessera region (study baseline is Ovda Regio) as well as first time measurements of important atmospheric species that can answer fundamental questions about the evolution of Venus. The ability to characterize the surface composition and mineralogy within the unexplored Venus highlands will provide essential new constraints on the origin of crustal material and the history of water in Venus' past. VITaL also provides new high spatial resolution images of the surface at visible and/or near infrared (NIR) wavelengths from three vantage points: on descent (nadir view), and two from the surface (panoramic view and contextual images of the linear surface chemistry survey). These data provide insight into the processes that have contributed to the evolution of the surface of Venus. The science objectives are achieved by a nominal payload that measures elemental chemistry and mineralogy at the surface, images surface morphology and texture on descent and after landing, conducts *in situ* measurements of noble and trace gases in the atmosphere, measures physical attributes of the atmosphere, and detects potential signatures of a crustal dipole magnetic field.

The team developed two basic design concepts that could survive landing in rough terrain: a low center of gravity Ring Lander, and an innovative cage design that uses gravity to orient the science payload after landing. The ring design is stable on lander scale slopes of up to 60° (from horizontal), allowing an additional 12.7° of dynamic motion upon landing. The Cage Lander can flip, but its successful operation is more complex. These capabilities are consistent with kilometer scale slope data for many tessera regions of <30° and allow for local 1.3 m high blocks. Either lander fits in an aeroshell with heritage geometry. Because the Cage Lander is more complex, the Ring Lander is considered the less costly of the two options, and is the baseline design chosen for costing. Significant trades were also conducted to assess crushable materials and active hazard avoidance. The thermal design uses phase change material that enables the lander electronics and instruments to survive 2 hours at the Venus surface, thus providing sufficient time for imaging and surface chemistry.

Launched on an Atlas V 551 in 2021, the carrier spacecraft delivers VITaL to Venus after an initial Venus flyby, which is required to achieve the appropriate landing conditions. After release from the carrier, the VITaL probe enters the atmosphere, briefly descends on a parachute, and then free-falls to the surface. Science is conducted on descent and at the surface. The total mission time in the venusian atmosphere is 3 hours, including 2 hours in the surface environment. VITaL transmits data to the flyby carrier spacecraft throughout the 3-hour science mission. After losing contact with the lander, the carrier S/C then relays all data back to Earth.

The most significant risks to a VITaL mission are related to development of a high TRL Raman/Laser Induced Breakdown Spectroscopy (LIBS) system, safe landing, and testing at Venus environmental conditions. To reduce risk, advancement in two key technology areas are needed: 1) verifying the Raman/LIBS implementation, and calibrated operation, and sizing for the Venus surface environment, including high entry loads on the laser, 2) additional analyses and testing to ensure safe landing in potentially rugged terrains (at lander scales). Although not required, a VITaL mission would benefit from additional high resolution topography and images to refine landing site selection.

1.0 SCIENTIFIC OBJECTIVES

1.1 Scientific Questions and Objectives

Venus is often referred to as Earth's sister because of their similar size and position within the solar system. Yet, despite their similar origins, the two planets have followed very different evolutionary paths. In the 1970s and 1980s, the plains regions were explored by multiple Soviet Venera Landers, and NASA launched the Pioneer-Venus mission (orbiter plus four atmospheric probes). The NASA Magellan mission (1990-1994) consisted of an orbiting spacecraft with a moderate resolution synthetic aperture radar and radar altimeter to globally map the surface. ESA's Venus Express (VEx) is currently in orbit observing polar cloud dynamics and composition, and JAXA is expected to launch Akatsuki in 2010 to monitor equatorial cloud dynamics and weather. In addition, Earth based observations using advanced polarimetric radar mapping have contributed significantly to our understanding of Venus.

The Deuterium/Hydrogen (D/H) ratio of the venusian atmosphere measured by Pioneer Venus and from Earth is the highest in the solar system, and is consistent with the loss of significant water over the history of the planet. Water is clearly unstable on the surface of Venus at present, and a lack of water in Venus' recent history has been invoked to explain why the planet may lack terrestrial-type plate tectonics. The ancient history of Venus, presumed to be more water rich, perhaps with an ocean and possibly habitable, can only be found in materials that predate the volcanic plains – these materials may be preserved in tessera terrain.

The key science driver for the Venus Intrepid Tessera Lander (VITaL) mission is to measure the mineralogy and major elemental composition of tessera terrain, which is distinct from the plains and is yet unsampled, and is essential to understanding the compositional diversity of the Venus crust. Tessera terrain consistently appears locally, and perhaps even globally, as the oldest material on a planet where the average surface age is ~500 million years. Thus, the tesserae provide the best chance to access rocks that are derived from the first 80% of the history of the planet, an era for which we currently have no information. Recent results from VEx and Galileo indicate that the highlands may have a higher surface albedo in the NIR than the basaltic plains, suggesting the highlands have a more evolved composition [Mueller et al., 2008; Hashimoto et al., 2008]. Evolved (silicic) compositions on Earth require both water-rich magmas and a plate recycling mechanism, neither of which is currently operating on Venus today but may have been in the venusian past. Thus, tessera terrain composition provides critical constraints on Venus geochemistry, geodynamics, and the history of water on the planet.

Near-infrared descent imaging below the clouds will provide a new dataset for Venus and enable a unique assessment of geomorphology and surface processes that can help calibrate the global Magellan radar and VEx image data. High resolution imaging of these unique terrains in optical wavelengths can provide details about the scales of geomorphic roughness and localized tectonic deformation, and possibly evidence of mass wasting in areas with topographic variability. Multispectral, panoramic imaging on the surface at the centimeter scale will constrain local morphology, stratigraphy, and weathering processes. Detailed contextual imaging of the surface where geochemistry measurements are made serves as the geologist's hand lens for assessment of mineralogy and rock textures.

Compositional measurements of the atmosphere constrain atmospheric evolution, but to date, very little compositional or physical information has been garnered about the lowermost scale height (<16 km), which is key to understanding both atmospheric evolution and surface-atmosphere interactions. Another objective of VITaL is to measure noble gases and their isotopes within the atmosphere, and to measure trace gases and their isotopes and physical parameters (pressure, temperature, and wind speed) at a new place and time on Venus through the atmosphere to the surface. These compositional measurements, particularly when combined with elemental chemistry and mineralogy observations on the surface, will provide an improved understanding of surface-atmosphere interactions, and may also potentially address the issue of active volcanism on Venus.

Finally, the status of the venusian interior is very poorly constrained. Orbital measurements show Venus to lack a magnetic field, which supports the conclusion that Venus lacks a dynamo at present. This result can be verified with surface measurements of any ambient field. Mantle overturn events, such as that hypothesized to have emplaced the Venus plains, may have been associated with an ancient active dynamo, traces of which may be present as remanent magnetism in Venus rocks.

1.2 Science Traceability

Table 1 traces the primary science objectives to the key measurements needed to address each. The third column of **Table 1** indicates nominal instru-

Table 1: Traceability of primary science objectives (in priority order) to functional mission requirements.

Science Objective	Measurement	Instrument	Functional Requirement
Characterize chemistry and mineralogy of the surface.	Major, trace elements, mineralogy, NIR spectroscopy	Raman/LIBS; NIR (1.0 micron) descent imager below 1 km, Raman/LIBS context camera	Access to tessera terrain, > 25 *in situ* sample measurements, sample context images
Place constraints on the size and temporal extent of a possible ocean in Venus's past	Measure D/H ratio in atmospheric water, mineralogy and major element chemistry of surface rocks.	NMS; TLS; Raman/LIBS	*In situ* sampling of the upper and lower (<16 km) atmosphere. Access to and measurement of tessera terrain.
Characterize the morphology and relative stratigraphy of surface units	Visible and NIR observations of multiple surface units at cm to m scale spatial resolution	NIR (1.0 micron) descent imager and surface panoramic camera with ~5 filters from 550-1000 nm.	Position of cameras to image the surface, while accommodating expected slopes, platform stability for clear images.
Determine the rates of exchange of key chemical species (e.g., S, C, O) between the surface and atmosphere	Measure trace gases in the near surface atmosphere, measure surface chemistry	NMS; TLS; Raman/LIBS	Repeated (every 100s of meters) *in situ* sampling of atmosphere, particularly below 16 km
Determine whether Venus has a secondary atmosphere resulting from late bombardment and the introduction of significant outer-solar system materials, including volatiles	Measure noble gases and their isotopes	NMS	*In situ* sample of atmosphere during descent.
Characterize variability in physical parameters of the near surface atmosphere (pressure, temperature, winds, radiation)	Temperature, Pressure, winds, atmospheric dynamics	Temperature, pressure, accelerometers, USO	*In situ* measurements of T/P throughout descent (every 10s of meters), communication with orbiter for Doppler winds
Place constraints on current levels of volcanism	Measure trace gases and isotopes in the atmosphere	NMS; TLS	*In situ* sampling of atmosphere through descent every 100s meters.
Measure ambient magnetic field from low- and near-surface elevations	Detection of existence or absence of magnetic signal	Magnetometer	Must be able to detect surface "signal" above payload "noise"

mentation that could satisfy the measurement requirements (see **Section 3.1** for details). Despite its different measurement capabilities relative to X-ray Diffraction/X-ray Fluorescence (XRD/XRFS), a laser Raman/Laser Induced Breakdown Spectroscopy (LIBS) remote sensing approach has been selected for surface elemental chemistry and mineralogy because it offers implementation advantages (i.e., absence of sample acquisition, handling, and transfer to an XRD/XRFS, and allowance for more sampling locations). Measurements of the mineralogy and major elemental chemistry of multiple tessera samples will capture local diversity and reduce measurement error. The very small sample size of the Raman/LIBS system (~300 micron spot) necessitates the design and incorporation of a high resolution camera, boresighted with the instrument, to characterize the Raman/LIBS targets and place them in geologic context. Descent and multispectral panoramic images of the landing site characterize surface morphology and variability in a terrain that has never before been examined at this scale or at optical wavelengths. Panoramic images spanning 240° around the lander help mitigate potential viewing obstacles that may be encountered if the lander comes to rest in locally rough terrain. Analysis of surface slopes in tessera terrain at the km scale shows that many regions typically have slopes <30° (**Figure 1**). VITaL is designed to survive slopes up to 60°, which is predicted to accommodate surface roughness on the meter scale (i.e., landing on a 1.3 m block on a 30° incline) as well as fault surfaces that are not well resolved in the currently available datasets.

The time required to collect multispectral panoramic surface image, chemical measurements of multiple targets and contextual sample location images, and the uplink of all data to the carrier spacecraft drives the operational lifetime of the VITaL to ~2 hours in the surface environment. The 2 hours of surface operations, combined with the ~1 hour of science on descent, flows to a nominal requirement for 3 hours of communication with the carrier spacecraft.

A typical Venus target landing error ellipse on the order of 75 km (E-W) by 150 km (N-S) is adequate for targeting tessera terrain, which is contiguous over hundreds to thousands of kilometers. An example landing site was selected in the continent-size tessera highlands of Ovda Regio. This near-equatorial site maximizes optimal lighting conditions for the descent images. A landing ellipse this size can access many regions within Ovda (see Appendix for alternative landing ellipses that meet the requirements) that are dominated by slopes <30° (at the kilometer scale) and avoid intra-tessera volcanic plains, which are not a desired chemical target. Improved knowledge of sub-kilometer surface hazards may place more strict requirements on landing precision.

1.3 Study Objectives

The science requirements driving the VITaL design are to 1) measure mineralogy and major element composition of multiple (>20) targets on surface rocks within tessera terrain and to provide contextual images of these targets, and 2) to collect nested images of the surface on descent and panoramic images around the lander. The final significant driver for this study is to develop a concept that minimizes mission cost and enables VITaL to remain in a New Frontiers cost envelope for the coming decade.

Tessera terrain has been recognized as a high priority target by VEXAG [Smrekar et al., 2009], and, as such, a tessera lander was included in the 2009 Venus Flagship study Design Reference Mission. That study concluded that the two most important technology development priorities were surface sample acquisition and rugged terrain landing. The VITaL mission design incorporates a Raman/LIBS system that successfully operates at the surface. This system has a capable laser and spectrometer optics path sized for the Venus CO_2 environment and based on comparisons with other proposed Venus Raman/LIBS systems (see **Section 3.1**, **Table 4**). The system enables collection of tens of measurements that provide a representative sample of a potentially heterogeneous surface target.

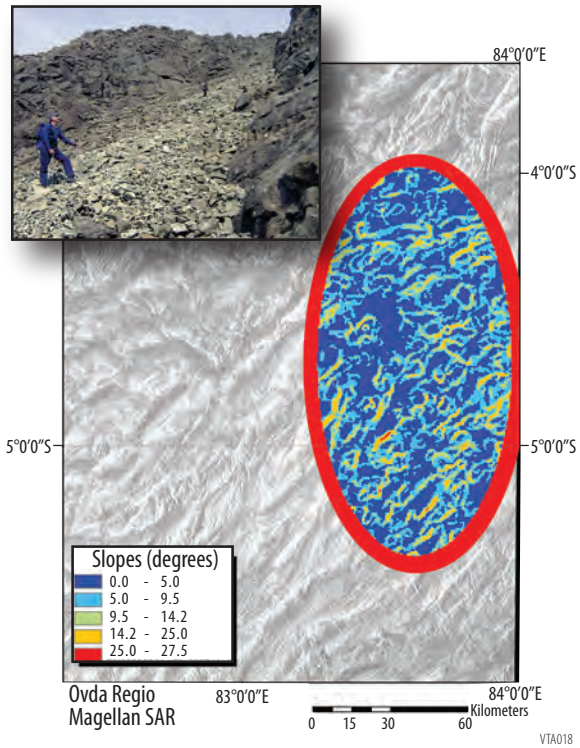


Figure 1: Synthetic Aperture Radar (SAR) and surface slopes in Ovda Regio. Slopes are calculated within an example VITaL landing ellipse of 75 X 150km. Slope data are derived from Magellan radargrammetry data (Herrick et al., 2010) and have a resolution of ~2 km. Kilometer-scale average slopes for this region are 6 ± 4° with a maximum slope of 28°. Slopes shown here are typical of tesserae generally. Inset: terrestrial example of ~20° slope. Fracturing of rocks and mass wasting may produce similar surfaces in Venus tessera highlands.

The primary challenges to landing on tessera terrain are surface roughness and slopes. These characteristics can be assessed using the Magellan altimetry data set (~10 km spatial resolution with ~80 m vertical precision), SAR images (75 m/pixel) and SAR radargrammetry data (~2 km spatial resolution). These data show average kilometer scale slopes in tessera terrain are ~5-10° and areas with slopes >10° are limited (0-5% of the surface; Figure 1, Ford and Pettengill, 1992; Ivanov, 2009). These data do not measure small scale faults observable in the SAR imagery. As on Earth, fresh extensional fault scarps are predicted to lie at 60-70° slopes, however, processes of mechanical weathering will serve to reduce these slopes to the angle of repose (~35°) on both planets. Measurements of 170 faults across Venus using radargrammetry yield an average slope of 36±2° [Connors and Suppe, 2001]. Even if all slopes on Venus tessera terrain were fresh, examination of a typical landing ellipse in Ovda (e.g., **Figure 1**) shows these slopes comprise only 1% of the landing ellipse. Meter scale roughness can introduce additional slope elements. Radar reflectivity data of tessera terrain is similar to that from terrains on Earth with roughness at the 10s cm scale [Campbell and Campbell, 1992, Arvidson et al., 1992], perhaps similar to the Venera 9 landing site, where a rock tilted the lander an additional 10° [Binsdschadler and Head 1989, Florensky et al., 1977]. As weathering on Venus is largely limited to mass wasting, tessera surfaces similar to scree slopes in arid regions on Earth are expected, where submeter scale rocks form talus deposits at the angle of repose.

While better (~100X) topography and imaging of potential landing sites will reduce landing risk, the VITaL mission is robust enough to tolerate tessera slopes ≤60°, which should accommodate 99% of expected slopes and rock sizes. A mechanical design that can land in any orientation is also presented. This trade is explored in **Section 3.4.1**.

2.0 HIGH-LEVEL MISSION CONCEPT

2.1 Overview

The VITaL mission design utilizes a concept carrier spacecraft and concept aeroshell and focuses on enabling landing in the rough tessera

landscape. Ovda Regio was selected to allow landing with a high sun angle (>45°) enabled by its location near the equator, though Alpha, Tellus, and Thetis tesserae may also be viable based on this criterion. The example shown in **Figure 1** indicates km scale slopes do not exceed 30° anywhere in a typical landing ellipse. The *in situ* instrumentation requires a lander that can assume known orientation with respect to the surface. Two classes of landers were conceived to meet this challenge. The Ring Lander was baselined as a focus for this study due to its relatively low complexity and its ability to fit the New Frontiers budget. The Cage Lander is discussed as a Trade (**Section 3.4.1**).

The VITaL Mission's space segments consist of a probe and flyby carrier spacecraft that is also used as a communications relay (**Figure 2**). The probe is comprised of two top level elements: the lander, and the Entry and Descent Element (EDE), which includes the aeroshell and parachute systems.

Carrier Spacecraft: The three-axis stabilized carrier spacecraft (**Figure 2**) performs three functions: 1) delivers the probe on an interplanetary trajectory to Venus, 2) releases the probe on an appropriately pointing trajectory to enter the Venus atmosphere, and 3) acts as a communication relay between the lander and the Earth. Because of the flyby trajectory, the required fuel mass is relatively small, thermal and power tasks are manageable, and electronics and communication systems are straightforward. The drivers for the carrier spacecraft design include spinning up the probe to 5 RPM prior to release and having a robust structure to support the probe. **Table 2** details the subsystem drivers for the Carrier Spacecraft.

Probe: The probe is released from the carrier 5 days before reaching the Venus atmosphere. The communications system is switched on 1 hour before encountering the atmosphere and transmits continuously. The aeroshell is designed with carbon phenolic material that ablates upon entry into the Venus atmosphere, where the probe experiences a deceleration of 200 g. The heat shield is jettisoned minutes after the parachute system on the backshell is deployed (at an altitude of ~60 km). Following this operation, the backshell and parachute system are released from the lander. *In situ* atmospheric structure, neutral mass spectrometer, and tunable laser spectrometer measurements are conducted throughout descent, and images are acquired from the NIR camera from ~15 km to the surface. The lander uses drag plates to slow the descent to the surface and crushable material to help absorb the kinetic energy of landing. Landing at 9 m/s produces an 86 g load on the pressure vessel. Once safely on the surface, the lander collects the Raman/LIBS measurements, Raman/LIBS context images, and panoramic images.

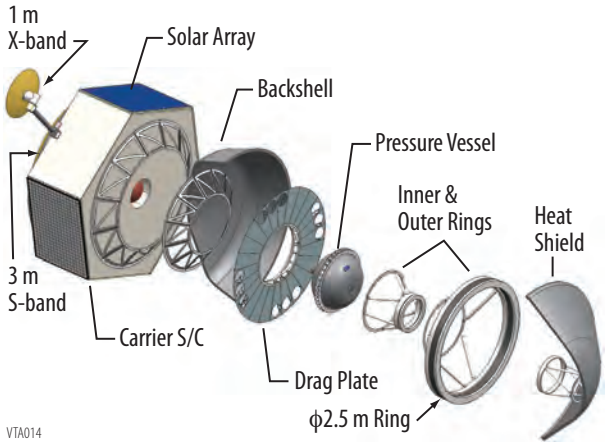


Figure 2: Carrier spacecraft and probe, exploded view.

Table 2: Carrier Spacecraft Complexity.

Subsystem	Brief Summary Of Concept	Complexity
Systems	Heritage spacecraft designs can be utilized, simple interfaces to Probe	Low
Flight Dynamics	Driving requirement to release probe on Venus entry interface trajectory	Moderate
Attitude Control Subsystem	Control SC with ¼ lb thrusters and spin up probe to 5 rpm with thrusters	Low
Propulsion	Delta V maneuvers relatively small for planetary missions	Low
Avionics	Low data rate	Low
Communications	Two antennas simplify operations; 3 meter lightweight S-band HGA to communicate with Probe and a 1 meter X-band HGA for communication with Earth	Moderate
Power	Low power needs allow for small solar arrays	Low
Mechanical	Driving requirement to minimize S/C mass, allowing for larger probe	Moderate
Thermal	Heritage thermal designs can be utilized	Low
Integration and Test	Most testing can be completed without probe, facilities exist for S/C testing	Low

2.2 Concept Maturity Level

Upon receiving the VITaL Study Questionnaire, a review of the current state of Venus all-terrain landers was performed. This review revealed the Concept Maturity Level was CML 2 or lower. Although probes to Venus have landed in the relatively flat volcanic plains, there are limited architecture trade studies on landers that evaluate cost, risk, or performance. The trade space was opened to all conceivable options for landing in any terrain. Initial evaluation of these options was conducted to determine their ability to satisfy the science requirements. After high level engineering evaluation, the options were narrowed to a Ring

Table 3: Instrument Resource Summary – the instruments in this table represent a notional instrument payload and to the extent possible, existing or proposed instruments were selected for which resources are known or have already been estimated.

	Mass (kg)	Power (W)	Volume (meters)	Data Rate/ Volume	TRL/ Heritage	Comment
Neutral Mass Spectrometer (NMS)	11	50	0.26 x 0.16 x 0.19	2 kbps	High/MSL/SAM	Data rate during descent; reduced to 33 bps on surface
Tunable Laser Spectrometer (TLS)	4.5	17	0.25 x 0.10 x 0.10	3.4 kbps	High/MSL/SAM	Data rate during descent; reduced to 300 bps on surface
Raman/Laser Induced Breakdown Spectroscopy (LIBS)	13	50	Per Optical Design	5.2 Mb per sample	Medium	12 bit, 3 measurements per sample - one Raman and 2 LIBS
Descent Imager	2	12	Per Optical Design	6.3 Mbits per image	High	12 bit, 1024 x 1024
Magnetometer	1	1	0.20 x 0.10 x 0.10	0.064 kbps	High/Various	Data rate during descent; reduced to 6.4 bps on surface
Atmosphere Structure Investigation (ASI)	2	3.2	0.10 x 0.10 x 0.10	2.5 kbps (descent) 0.25 kbps (surface	High/Flagship	
Panoramic Imager	3	12	Per Optical Design	16.4 Mbits per band	High	12 bit, 2048 x 2048 detector
Context Imager	2	12	Per Optical Design	25.2 Mbits	High	12 bit, 2048 x 2048 detector

Data volumes include 2:1 compression

Lander and a Cage Lander (see **Section 3.4.1**.) The baselined Ring Lander meets the Inner Planet Panel's VITaL science objectives. The Cage Lander requires further development to overcome design issues highlighted in **Section 3.4.1**. The Ring Lander concept can be successfully completed within the mass requirements of an Atlas V launch vehicle, land in rough terrain, and demonstrates that power and thermal systems can be fabricated to survive for >2 hours in the Venus environment. While significant engineering design is still needed, the VITaL study shows no major technology development is required to support this mission. All components are TRL 5 or above.

The preliminary risk assessment encompasses the major developmental and operational risk areas and outlines necessary actions to reduce or eliminate these risks. The concepts described in this report raise the Venus all terrain lander to CML 4, Preferred Design Point, for the Ring Lander concept.

3.0 TECHNICAL OVERVIEW

3.1 Instrument Payload Implementation

Table 3 lists the science instrument payload identified in the Science Traceability Matrix (Table 1) and shows the accommodation resources required for each instrument. Specific implementation is left to future individual mission designs. Designs of the four optical instruments are provided in **Section 3.2.4.5**. TRL assessments of low are below 4, TRL assessments of medium are 4 or 5, and TRL assessments of high are 6 or above.

Neutral Mass Spectrometer (NMS): provides *in situ* measurement of noble gas isotopes and multiple trace gas mixing ratios. The NMS instrument consists of three modules: an ion source to convert gas phase sample molecules into ions; a mass analyzer, which applies electromagnetic fields to sort the ions by mass; and a detector, which measures the abundance of each ion present. Gas samples are ingested through gas inlet ports in the bottom of the pressure vessel. Due to the difficulty of exhausting gas to an 81 bar environment, exhaust sample gas is captured in a reservoir inside the instrument.

Tunable Laser Spectrometer (TLS): measures trace gases, including multiple isotopes of sulfur and hydrogen-bearing species. Of particular interest, the TLS measures the Deuterium/Hydrogen (D/H) ratio in atmospheric water via measurement of molecular line parameters for infrared molecular absorption lines. Utilizing extremely small tunable laser spectrometers with room-temperature laser detector arrays in a Herriott cell configuration, TLS provides multi-wavelength *in situ* measurements of the Venusian atmosphere. Gas inlet ports at the bottom of the pressure vessel feed sample gas into the Herriott cell; the number and detailed implementation of the NMS and TLS gas inlet ports can be determined by future mission designs. Exhaust sample gas is captured in a reservoir inside the instrument. TLS is combined with the NMS, sharing common electronics and piping, but is listed separately since each spectrometer has unique measuring timelines.

Raman/Laser Induced Breakdown Spectrometer (LIBS): is a combined instrument, utilizing a single laser and a single telescope to provide mineralogy and elemental chemistry of surface rocks. Raman illuminates the remotely located (~2 to 3 m) sample with a low power 532 nm laser pulse and observes the scattered return (Raman wavelength shift) to determine the vibrational modes of

Table 4: Sizing Scale of Baseline Raman/LIBS versus other Studies of Raman/LIBS systems

Reference	1064 nm energy LIBS (mJ)	532 nm energy Raman (mJ)	Distance (m)	Telescope Dia (cm)	Analytical Spot Size (mm)	Telescope Dia^2 x Laser Energy / (Distance^2)	Ratio with Sharma	Frequency (Hz) (Raman/ LIBS)	Power (W)
Sharma, et al.	50.0	15.0	1.5	12.7	0.25	3584.2	1.0	0.5	
Clegg, et al.	50.0	35.0	1.7	12.7		2891.6	0.8	10.0	
Wiens, et al.	50.0	35.0	8.6	12.7	0.60	109.0	0.0	20.0	
Baseline	**50.0**	**15.0**	**2.5**	**6.5**	**0.30**	**338.0**	**0.1**	**20.0**	**50.0**

In Red, Assumed Diameter

the chemical bonds in the target. LIBS utilizes this same laser at a higher power level (1064 nm) to vaporize and ionize a portion of the target material, creating a plasma. By measuring the intensity and wavelength of the photons emitted by the plasma, the elemental chemical composition of the sample is inferred. The instrument accesses the sample area through a viewing window on the side of the lander and requires a 6.5 cm clear aperture.

The Raman/LIBS spectrometer is designed to have a 300 micron spot size and receiver. The focal point of the spectrometer utilizes a 3000 x 96 pixel CCD. The spectrometer and context camera are mounted on a bench that pans +/-10°. The 20 Hz source laser provides 15 mJ of 532 nm and 50 mJ of 1064 nm focused illumination. The size of the laser and receiver are scaled up from Mars Science Laboratory ChemCam and ExoMars versions of these instruments, though they are less sensitive compared to other studies of Raman/LIBS applications at Venus (**Table 4**). This sizing increase versus Mars missions is to account for the attenuation of the Venus CO_2 atmosphere. The laser is coupled to the common optics with a flexible optical fiber link. Landing in the tessera will result in uneven slopes and unpredictable distances between the lander and the measured rocks. Therefore a mechanism is built into the optical train that moves the common (to the receiver and laser source) primary mirror to enable the laser and receiver to focus anywhere from 2 to 3 meters away (this only requires +/-5 mm of travel which could easily be expanded). Focus is achieved by comparing return signal strengths. Raman/LIBS measurement locations are outside the outer landing ring and within the FOV of the panoramic camera (**Figure 3**). Six inches of clearance are allowed above the outer ring to enable some unplanned plastic deformation of the ring due to adverse landing conditions.

Raman/LIBS Context Imager: is co-aligned with the Raman/LIBS spectrometer. The spectrometer optics and the imager are located on a rotatable bench. The imager utilizes its own 3 cm viewport. The Raman/LIBS context camera has a narrow field of view of 4.6° x 4.6° (20 cm x 20 cm spot at 2.5 meters). This imager captures the geological context of the Raman/LIBS measurements. Its FOV overlaps with the panoramic camera (**Figure 3**) and descent images are also referenced. Future studies will need to address potential interference from dust disturbed at touchdown, particularly the possibility of dust adhering to the window.

Descent Imager: points in the nadir direction and acquires images during descent (**Figure 3**). Images of the Raman/LIBS sample area are recorded during the final moments of descent, providing additional information about the site prior to landing. The camera requires a 2.4 cm viewing window. The camera optics provide a 40° x 40° FOV with a 1024 x 1024 array, resulting in 0.84 m pixel size at 1 km.

Panoramic Imager: points along the horizon in four orthogonal directions and acquires images once landing has occurred. The panoramic camera has a mechanized filter wheel with five filters and one neutral density filter. The filters are 550, 650, 750, 850, 1000 nm, each with bandwidth of 20-30 nm. The camera has a FOV 25° below the horizon and 10° above the horizon by 60° wide (**Figure 3**). Four windows in the cupola on the top of the pressure vessel enable a 240° view. A mechanism within the pressure vessel rotates a mirror to allow the camera to sequentially acquire images through each of the four windows (mechanisms are discussed in **Section 3.2.4.3**). One of the panoramic windows has a clear view of the Raman/

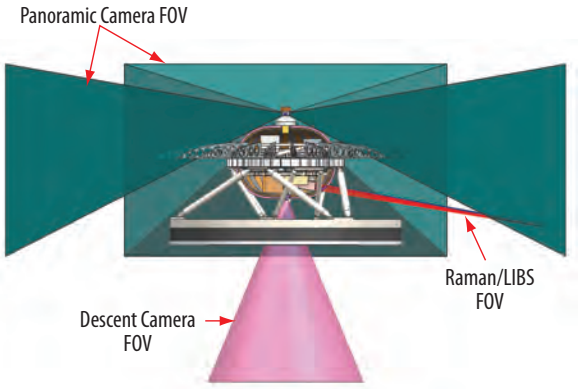


Figure 3: Fields of View for cameras and Raman/LIBS VTA015

LIBS measurement locations with a pixel resolution of 0.4 cm at a 3 m distance. Like the Raman/LIBS context imager, future studies will need to address potential interference from dust disturbed at touchdown, particularly the possibility of dust adhering to the window, though being located on the top of the lander on the other side of the drag plate should decrease this sensitivity.

Triaxial Fluxgate Magnetometer: determines the presence or absence of a planetary magnetic field. This instrument is inside the lander; no boom is required. This is sufficient, since planetary and/or local rock magnetic fields of interest are orders of magnitude larger than typical electronics fields.

Atmospheric Structure Investigation (ASI): has sensors located on the outside of the lander to characterize gross atmospheric properties, including temperature and pressure. This package consists of a temperature sensor, a pressure transducer, anemometer, and an accelerometer. The nominal implementation concept does not utilize a boom or mast; exact implementation of this instrument package is left to a future study. The VITaL science payload operations concept is detailed in **Section 3.2.1**.

3.2 Flight System

3.2.1 Concept of Operations and Mission Design

A 20-day Type II launch window in 2021 was analyzed for launch on an Atlas V 551 (the Russian Proton-M launch vehicle would also be feasible). The launch window meets the launch mass (with a C3 of 8.8 km^2/sec^2) and probe entry interface velocity constraints as well as the Ovda Regio landing site location and illumination constraints. A Venus re-encounter trajectory with an initial flyby and a second Venus encounter approximately 112 days later ensures the landing site location and illumination constraints are met across the launch window. After releasing the probe 5 days prior to the second Venus encounter, the spacecraft performs a Venus flyby and receives data throughout the lander science mission. The timeline of significant events for the November 2, 2021 launch trajectory is shown in **Table 5**. Additional trajectory options could be investigated, including identification of viable launch windows during the next opportunity in 2023 that could land in a tessera region.

Table 5: VITaL Significant Events for November 2nd Launch

Launch Window Open	October 23, 2021
Launch	November 2, 2021
Launch Window Close	November 11, 2021
Venus Flyby	April 7, 2022
Probe Separation	July 24, 2022
Carrier Divert Maneuver	July 25, 2022
Landing	July 29, 2022
Carrier Playback of Lander Data	July 30, 2022
End of Mission	August 6, 2022

Three spacecraft trajectories during lander entry and descent were considered for the second Venus encounter: two Venus flyby trajectories and one Venus Orbit Insertion (VOI) trajectory. One flyby option was determined to be the most desirable (based primarily on spacecraft-lander range data and fuel mass requirements), and is the option used in this study. Table 6 summarizes the selected 2021 launch window. The window open and close cases are patched conic. The middle of window trajectory (November 2, 2021 launch) was an integrated trajectory used for detailed analysis and included Solar, Earth, Venus, Lunar, and planetary gravity, Solar radiation pressure, and Venus drag; this integrated middle window trajectory was consistent with the patched conic case, as expected. The absolute value of Declination of Launch Asymptote (DLA) is below 28.5° and the minimum Venus flyby altitude is 6,475 km for all launch opportunities in **Table 6**.

A delta-V budget including statistical and deterministic delta-Vs and margin was determined for the November 2, 2021 launch opportunity. The delta-V requirement is 156 m/s before probe release and 126 m/s after.

Figure 4 is a Venus-centered view of lander entry interface and the spacecraft flyby on July 29, 2022. Landing occurs ~2° downrange of the entry interface. The 2021 launch window results in a landing at Venus IAU latitude S 8.5°, longitude E 85.0° in Ovda (e.g., Figure 1), with a Sun elevation at the landing site of ~65° (where 90° is the subsolar point). This opportunity satisfies the re-

Table 6: 2021 Launch window parameters (Type II trajectory)

Launch	Venus Flyby	Landing	Launch C3 (km^2/s^2)	Hyperbolic Excess Velocity at Lander Entry Interface (km/s)	Lander Entry Interface Velocity at 175 km Altitude (km/s)
October 23, 2021	April 5, 2022	July 27, 2022	8.01	4.79	11.3
November 2, 2021	April 7, 2022	July 29, 2022	7.92	4.78	11.3
November 11, 2021	April 10, 2022	August 1, 2022	8.88	4.82	11.3

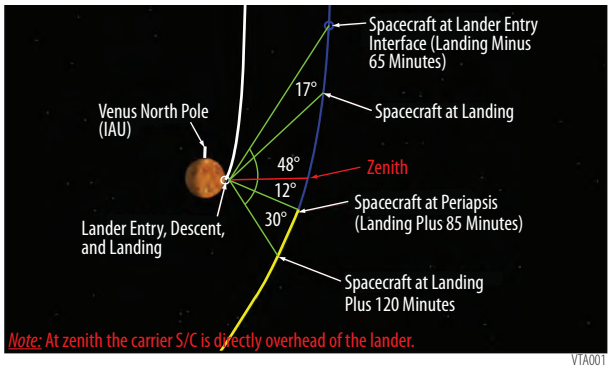


Figure 4: July 2022 Flyby geometry during probe entry, descent and landing.

quired greater than 45° sun angle for NIR images. Flight dynamics solutions were not optimized for specific, precise target landing locations during this study. Some flexibility in landing locations exists. The landing longitude can be varied approximately 44° around the subsolar point. Small changes on the order of degrees in the landing latitude can be achieved with the current design. Substantial changes in latitude require modification of the entry and descent design resulting from changes in the entry angle. The spacecraft divert delta-V and spacecraft-lander range and elevation profiles for these modified landing locations would be similar to those included in this study report.

Operations at Venus are autonomous, based primarily on time relative to specific events. The probe is in a low power mode during the five-day coast after separation from the carrier spacecraft. Daily brief telemetry transmissions to the carrier spacecraft are performed to enable the carrier spacecraft to verify pointing to the probe. The communications system turns on one hour before predicted atmospheric entry to ensure adequate time to adjust carrier pointing, if necessary; the probe transmits continuously for the next 4 hours.

The aeroshell protects the lander during atmospheric entry. After the probe has slowed (~1 minute), the drogue parachute and then the main parachute are deployed, extracting the lander from the heat shield. The parachute is then released, and the lander free-falls to the surface. The lander will have enough drag to spend > 60 minutes in the descent to allow time for the atmospheric measurements and to drop to the surface at a velocity < 9 m/s.

Figure 5 illustrates instrument operations during descent. The magnetometer and the internal components of the Atmospheric Structure Investi-

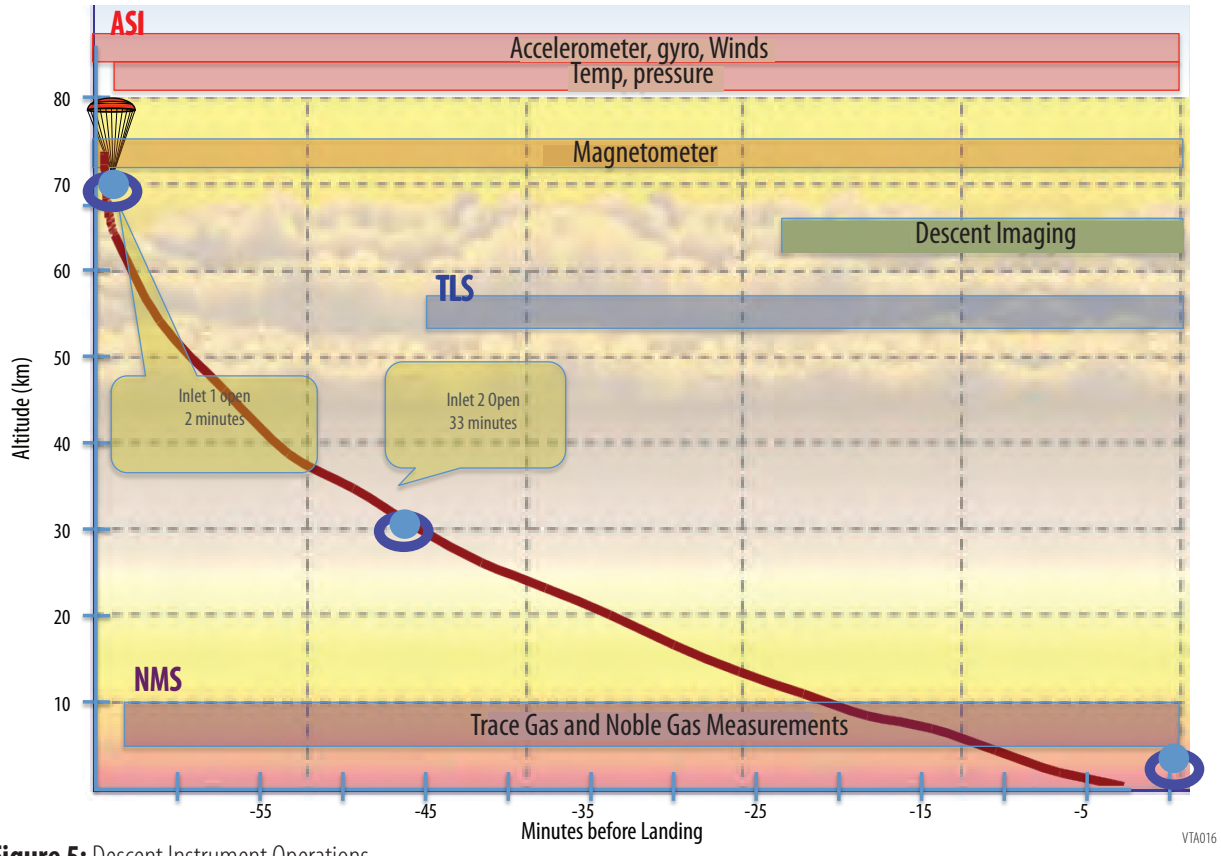


Figure 5: Descent Instrument Operations

gation (ASI) operate from above the atmosphere to the end of the mission. The NMS and the external components of the ASI start operations as soon as the aeroshell is released. The NMS performs trace and noble gas analysis during descent using an external atmospheric inlet port. The TLS operates from below the clouds to the surface.

The Descent Imager starts imaging between 15 and 20 km above the surface, buffering the 12 bits per pixel images. The murky atmosphere and motions of the lander will affect image quality during descent; a 1 ms exposure time helps mitigate the motions. All images are stored in memory; higher quality images are selected and uplinked. The nominal number of descent images is 15 for uplink (**Figure 6**).

Instrument operations after landing are shown in **Figure 7**. The ASI, NMS, TLS, and Magnetometer instruments reduce their duty cycle after landing. The Raman/LIBS instrument immediately begins surface analysis. It samples up to 60 locations along a 0.86 meter survey line (**Figure 8**) (assumes the surface is 2.5 meters from the instrument window). The Raman/LIBS points to the sample location, focuses the instrument, performs one Raman measurement and two LIBS measurement, and then moves to the next location. The duration at each location is about 2 minutes. The co-aligned Context Imager takes an image at each location. Five of the full images are downlinked to provide complete coverage of the sampling site (**Figure 8**). In addition, small (100 x 100 pixel) sub-images in the center of the image are downlinked for each sample to provide precise knowledge of the sample location.

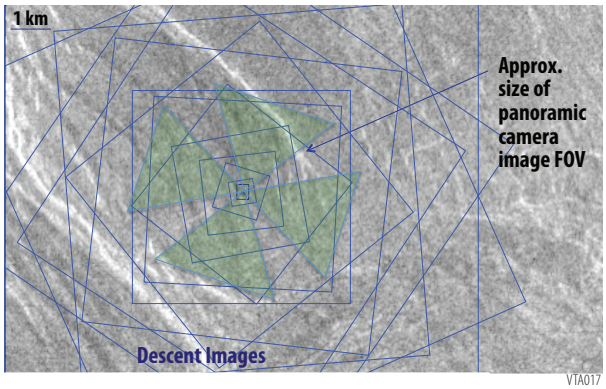


Figure 6: Descent and Panoramic Imagery

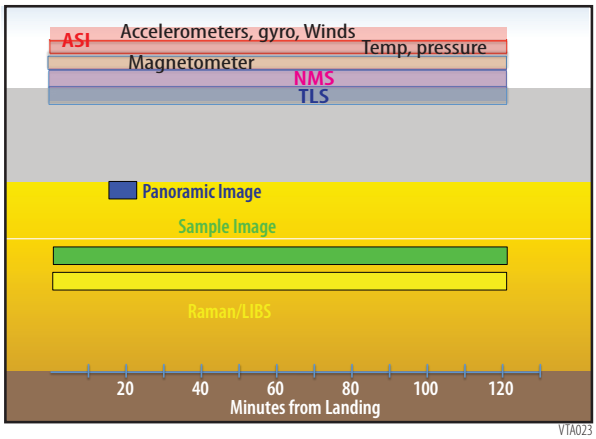


Figure 7: Surface Instrument Operations

The Panoramic Imager begins taking images 15 minutes after landing (to allow time for dust to settle). Panoramic images are acquired using six filters at each of four different angular locations for a total of 24 images.

Since the communications system varies the data rate based on the signal strength to the carrier, the amount of data returned depends on the angle with respect to the flyby spacecraft. Data uplink begins during descent. If the landing location is horizontal (0° inclined), the link returns 964 Mbits from atmospheric entry through 2 hours on the surface (**Figure 9b**). If the lander is inclined 40° relative to the flyby spacecraft, antenna gain is reduced and 723 Mbits are returned (**Figure 9a**). The data rate is autonomously negotiated between the spacecraft and lander. The spacecraft monitors its decoder statistics and commands the data rate higher or lower to ensure reliable communications. A similar scheme is currently implemented in the Electra equipment used between payloads on the surface of Mars and Martian orbiters. The lander buffers the data and sends the highest priority first. In the 40° case, the lander sends 75% of the panoramic images and 65% of the Raman/LIBS measurements. This drops to 356 Mbits or 37% of the total if the angle is 60°; the rate meets the minimum science requirements if this worst case slope is realized.

The lander is designed to operate for 2 hours after landing. At the end of the 2 hours, the lander continues to send buffered images and replays high priority data for as long as it and the communication link lasts.



Figure 8: Raman/LIBS sample locations (yellow dots) and context images.

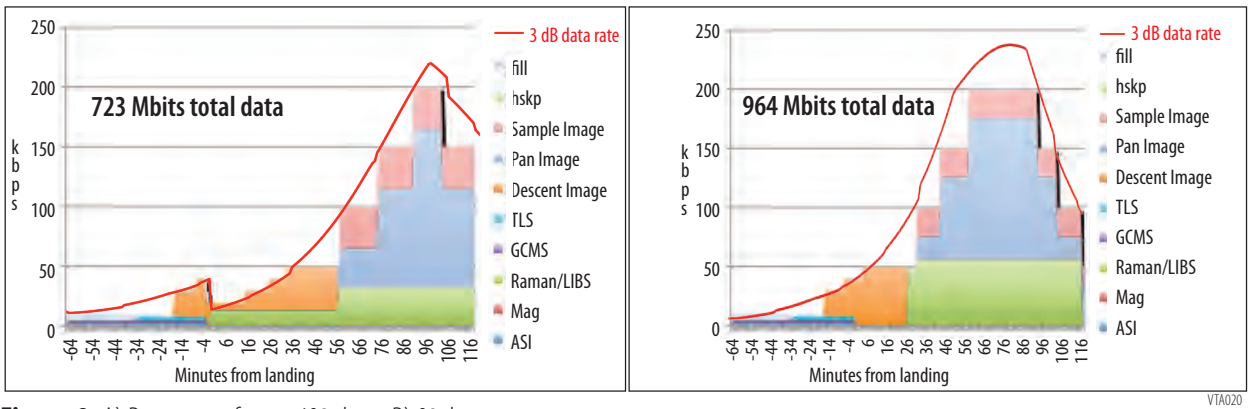


Figure 9: A) Data return from a 40° slope, B) 0° data return

3.2.2 Carrier Spacecraft

The carrier spacecraft is three-axis stabilized. Spacecraft mass is dominated by the structure required to support the probe; the remaining subsystems are modest. Carrier spacecraft details are provided in **Table 7**.

The spacecraft power Current Best Estimate (CBE) budget is provided in **Table 8**. The contingency for power growth is held in an oversized solar array. 3 m^2 of solar arrays are body mounted. The secondary (rechargeable Lithium-ion) battery is manageable, as no significant eclipse is expected, though its size is driven by off pointing to enable lander-to-carrier and carrier-to-Earth communications. Even though it will experience ~1.9 suns, the solar array will stay below 140° C with Optical Solar Reflectors (OSR) tiled within the Solar Panel. Approximately half the delta-V budget of 270 m/s is used before probe release and half is used after for the carrier's divert maneuver. A hydrazine system is baselined.

The carrier communication sub-system includes a 3-meter low mass mesh S-band antenna for uplink communication with the probe, and a smaller 1-meter solid X-band antenna for downlink Deep Space Network (DSN) communication. The 3-meter HGA size reduces the uplink RF power requirements on the lander. The carrier's pointing requirement for carrier-to-lander communications is within 0.8°. When data from the probe are fully uploaded, the carrier spacecraft re-orients to point the 1-meter fixed X-band HGA within 0.2° of the DSN ground station, and downlinks at 25 kbps. Two X-band omni-directional antennas allow the carrier spacecraft to be commandable at all times. Because Ka-band omni-directional antennas have yet to be demonstrated, for this study, X-band was assumed for all communications with Earth. The cost to develop Ka-band omni-directional antennas is modest and would enable carrier-to-Earth communications to use Ka-band if driven by DSN 2021 capabilities, as suggested by the study ground rules.

Table 7: Carrier Mass Budget (CBE) with growth allocation of 30%

Sub-system	Mass	Margin	Total
Probe Separation System	30	30%	39
S/C Mechanical, Structural	506	30%	658
GN&C	11	30%	14
Propulsion Hardware	55	30%	72
Thermal	60	30%	78
Power	28	30%	37
Harness	31	30%	40
RF Comm	50	30%	65
Avionics	45	30%	59
Launch Vehicle Separation System SC side	30	30%	39
Spacecraft Mass Total (masses in kgs)	**846**	**-**	**1100**

3.2.3 Entry and Descent Element

The Entry and Descent Element (EDE) is composed of the aeroshell, parachute, and deployment mechanisms. The EDE provides aerodynamic drag during entry and also protects the probe from entry heating. The aeroshell structure and thermal protection system (TPS) materials are designed to sustain the high deceleration loads (~200g during entry). Sensitivity studies were performed for the VITaL mission parameters based on scaled versions of the Pioneer Venus Large Probe (PVLP). The -23.35° Entry Flight Path Angle (EFPA) and entry velocity of 11.3 km/s were selected to minimize g-loads

Table 8: Carrier Power Budget (CBE)

	Launch	Cruise	Probe Cruise
S/C Total	171	304	304
GN&C	50	50	50
Propulsion Hardware	1	1	1
Thermal	0	90	90
Power	10	20	20
Harness	3	6	6
RF Comm	20	50	50
Avionics	87	87	87

All Numbers in Watts

(for ease of qualifying instruments and minimizing the structural mass of the aeroshell structure) and total heat load on the heat shield (for minimal TPS mass). After withstanding peak deceleration and heating, the parachute is deployed at 60 km, and the heat shield is separated from the lander using explosive separation bolts. Finally, the parachute and backshell are severed from the lander element, completing payload extraction. The monocoque 3.5 m diameter, 45° sphere cone aeroshell, shown in **Figure 10**, encapsulates the lander, supports launch and entry loads, and enables safe and reliable atmospheric extraction of the lander. The heat shield is a scaled version of PVLP (which was 1.42-m diameter), while the back shell is similar in shape to Stardust. The structure is a 2-inch (5.08 cm) sandwich configuration with composite face sheets and aluminum honeycomb, providing mass savings over solid aluminum with sufficient structural integrity up to 225 g. The total mass of the aeroshell, including structure, TPS, and parachutes, is 1050 kg (not including 30% margin). The heat shield's mass is 717 kg, the back shell's mass is 293 kg, and the parachute and mechanisms are 50 kg. The heat shield TPS consists of 0.93 inch (2.325 cm) total tape wrapped and chopped molded carbon phenolic (TWCP and CMCP) onto the honeycomb structure. CMCP and TWCP are the only materials flight-qualified for the severe conditions of Venus entry. Peak stagnation heat flux (combined convective and radiative) on the heat shield is calculated to be 4.6 kW/cm^2 (2021 launch). Both CMCP and TWCP were flown on the Pioneer-Venus and Galileo entry probes. Although heritage carbon phenolic (CP) production has been discontinued since the 1980s because the supplier ceased production of the rayon precursor, Ames Research Center (ARC) has a sufficient supply of the original CP precursor to fabricate a VITaL-sized probe and the associated test and evaluation billets. Even assuming a PVLP-sized probe is launched to Venus prior to VITaL, there is sufficient heritage rayon to construct the VITaL aeroshell (see Appendix).

Based on engineering estimates for the backshell environment, Phenolic Impregnated Carbon Ablator (PICA), a light weight ablator, can be used as the back shell TPS material. The PICA tiles are bonded to the structure using HT-424, with RTV-560 filled gaps, using the same manufacturing techniques as Mars Science Laboratory (MSL). PICA has flown on Stardust and has been extensively evaluated and characterized as a heat shield material for MSL and was a candidate heat shield for Orion.

3.2.4 Lander

3.2.4.1 Lander Structure

Mechanical Overview

The mechanical system is designed to safely transport the instrument suite to a tessera region on the Venus surface. The mechanical design of the lander concept (**Figure 11**) is driven by the two most challenging requirements: the high deceleration loads expected during entry into the Venus atmosphere, and operational stability of the system after landing on an unknown terrain. Due to the uncertainty about terrain conditions at the landing site, proposed designs were selected to provide a high level of assurance of success even if the terrain is extremely uneven. It was assumed that the worst case scenario for this design

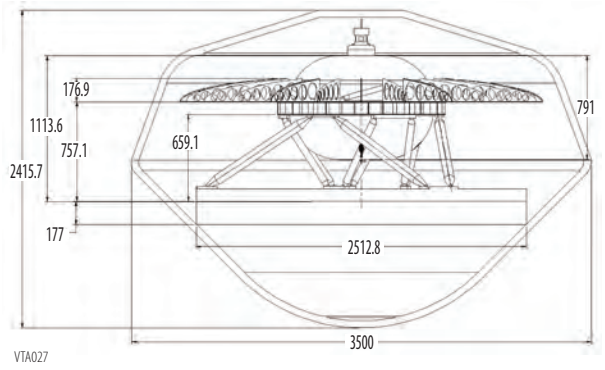


Figure 10: Aeroshell Dimensions (in mm)

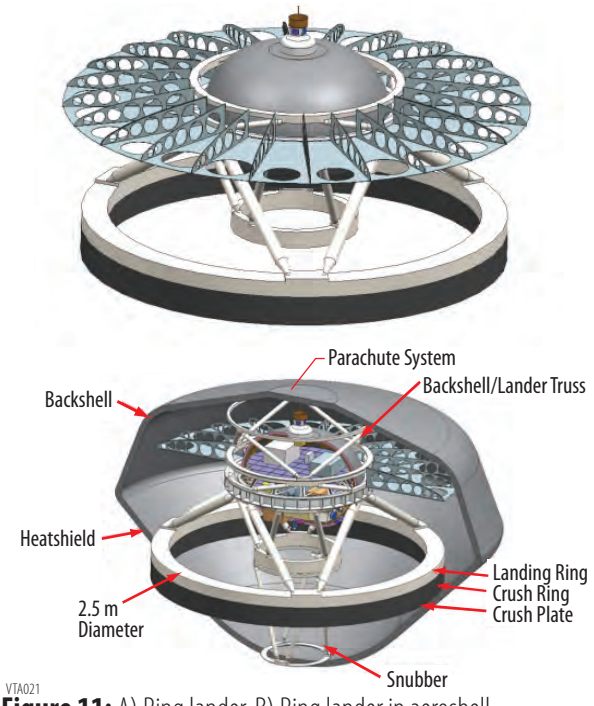


Figure 11: A) Ring lander, B) Ring lander in aeroshell

was landing on a 30° slope and with the high side of the lander striking a 1.3 m high block.

The Ring Lander design meets the instrument suite field-of-view (FOV) requirements for ground imaging during descent and landing, and for the Raman/LIBS instrument (**Figure 3**). The panoramic camera FOV requirement is met using the cupola structure at the top of the pressure vessel (**Figure 3**), and must include the Raman/LIBS sample location. The concept also meets the TLS and NMS instrument requirements for small vent openings by employing a 5 mm diameter vent opening with frangible ceramic solenoid actuated caps for atmospheric sampling.

The structural system design accommodates the high performance thermal control system, which includes isolation and insulation systems and phase change materials. The probe primary structure is a hermetically-sealed pressure vessel to reduce the transfer of thermal energy and prevent the influx of Venus atmosphere. The entire packaged lander is designed to fit into an aeroshell system (**Figure 11b**) and survive the 200 g loads expected during entry into the Venus atmosphere and the 83 g loads expected at impact on the Venus surface.

Stability of the lander is based on a high-mass outer ring, lowering the center of gravity and providing a stable base upon landing. The design also includes an inner ring to protect the probe from protruding objects during landing. The inner ring is recessed from the main landing ring and may require some crushable material depending upon the analysis. The current design concept has a static tip-over stability of up to 72.7° (**Figure 12**). The system allocation for this static tip angle is: 30° for macro scale slopes, 30° for a 1.3 m block, 10° for dynamic landing conditions, and 2.7° unallocated (**Figure 13**).

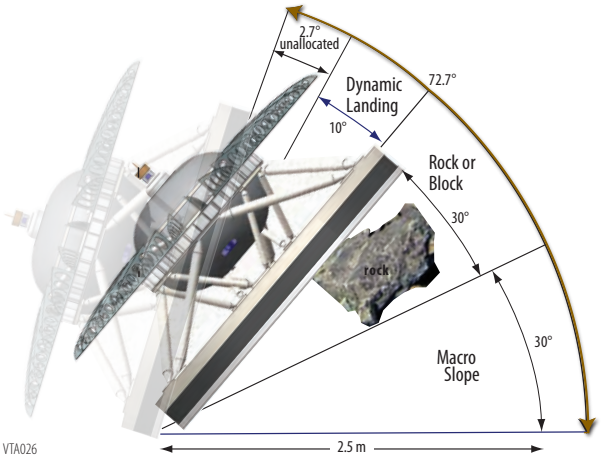


Figure 12: Ring design maximum static stability

Load Paths

The primary loads on the system occur at launch, entry, and landing. The launch loads are carried on hard points in the backshell. A releasable truss or legs support the lander through the backshell. This structure also provides a way to support the lander as it hangs beneath the backshell after the aeroshell has been released. The release mechanisms drop the lander from the backshell for the freefall landing.

The primary structure was designed to handle the 200 g deceleration loads on the probe during the Venus atmospheric entry phase of mission timeline and a 9 m/s expected impact velocity for landing. The design provides deceleration using a crushable titanium foam ring that reduces the expected landing loads to 83g.

For the high entry loads, the design relies upon a snubber system. The snubber is not mechanically joined to the lander, but during entry, the lander flexes into contact with the snubber, transferring loads to the aeroshell. This eliminates the need for excessive bridging structure or mechanisms to carry the entry loads and provides thermal isolation during all the other phases of the entry, reducing thermal gain through the aeroshell.

The design relies upon crushable titanium foam and support legs to absorb the landing impact. The legs could also include a collapsible piston design, increasing the amount of stroke and energy absorption and thereby decreasing the g-loads during landing.

Packaging

All major components can be accommodated in this design with volume margin for inevitable growth and the addition of secondary components that were not considered for this study (**Figure 14**). The pressure vessel volume was not

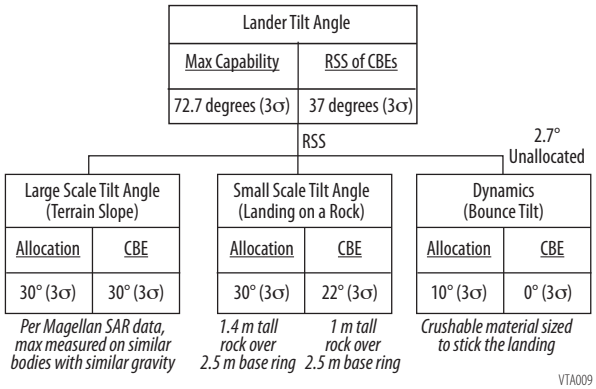


Figure 13: Lander tilt allocation budget

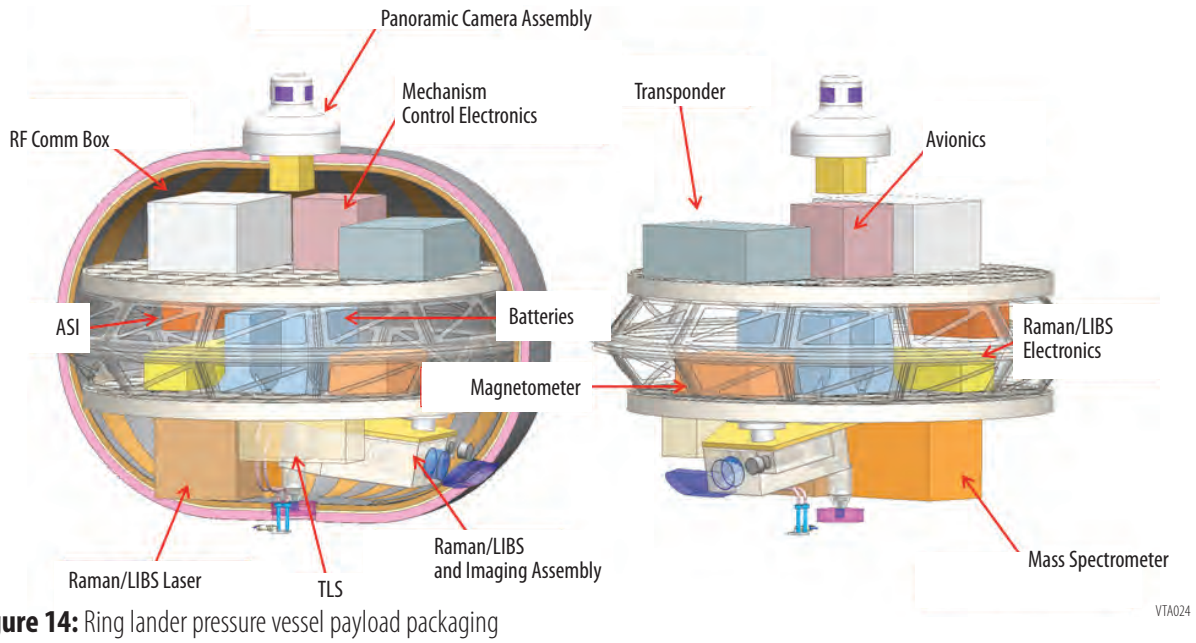


Figure 14: Ring lander pressure vessel payload packaging

optimized, and some adjustment will likely be necessary as the design matures. Currently, the probe is well within the constraints of the aeroshell volume and there are no obvious issues for accommodating the payload.

Materials and Mass Properties

The extremes of the environment and the high g-loading drove the choice of a default material for the structural concept to titanium. Commercially available (high void fraction and vented) titanium foam is used for the crushable material. Preliminary sizing of the structural elements was performed to estimate sizing and to demonstrate concept feasibility. Detailed aerodynamic analysis of the drag plates was not performed, but the coefficient of friction was estimated from assuming the lander had a disk profile (based on the drag plate shape) and calculating Reynold's number to determine the terminal velocity. The complex dynamics of impact for the design is beyond the scope of this study but preliminary analysis indicates that the concept appears feasible. The drag plates shown in Figure 10 are 2.5 m in diameter. The aeroshell can accommodate drag plates up to 3.2 m in diameter, which will lower the impact velocity to 7 m/s.

Table 9: Analysis plan

Design Goal	Lander Details	Notes
Fund. Freq (in aeroshell)	>35 Hz	Engineering judgment
Atmospheric Entry Load	200 g	Calculated
Landing Velocity	10 m/s	Calculated (CBE is 9 m/s)
Level Landing Load	83 g	Derived
Non-level landing load	43 g	Derived

3.2.4.2 Lander Mechanical Static and Dynamic Analysis

Analysis Goals

The Ring Lander has been analyzed to verify that the design concept meets structural load and stability requirements during atmospheric entry and landing. Loads and stiffness requirements were both assumed and derived. The basic load cases are atmospheric entry, level landing, and landing on a macro and micro slope (40° inclined assumed). **Table 9** shows the load cases analyzed. The analysis used a landing velocity of 10 m/s, though for the actual lander, this was calculated as 9 m/s.

Landing Load Calculations – Ring Lander

A crush pad area and depth were calculated based on the amount of crush material needed to absorb the full kinetic energy of the lander upon contact with the surface. **Figure 15** illustrates how the crush pad area (as a percentage of the lander ring area) relates to crush pad required depth and the resulting equivalent g loading.

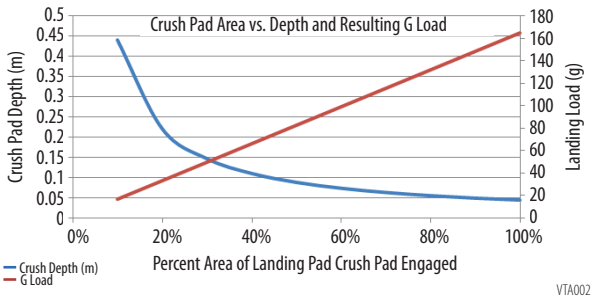


Figure 15: Percent Area of Landing Pad Engaged

For the flat landing case, it was assumed that a crush pad covering 50% of the lander ring was engaged. For the non-level case, it was assumed that an area of 25% was engaged. This assumed that a load spreading plate under the crush pad helps distribute the load over a greater area of crushable material.

With the assumption that the crush pad absorbs all the energy from the landing, it can also be inferred that the lander will remain upright as long as the system CG is low enough to be within the diameter of the landing ring. Calculations show that for the given CG location and lander ring diameter, the system is stable up to an angle of 72.7° versus the 60° requirement.

Analysis Models and Results

The Ring Lander was modeled in the MSC/NASTRAN finite element analysis software and the design was analyzed to verify that primary structure meets ViTaL loading and stiffness goals (**Table 9**). **Figure 16** shows the model used in the analyses. Only the primary and major secondary structural elements were analyzed for this effort. The pressure vessel and internal components are represented as simplified mass elements for the model.

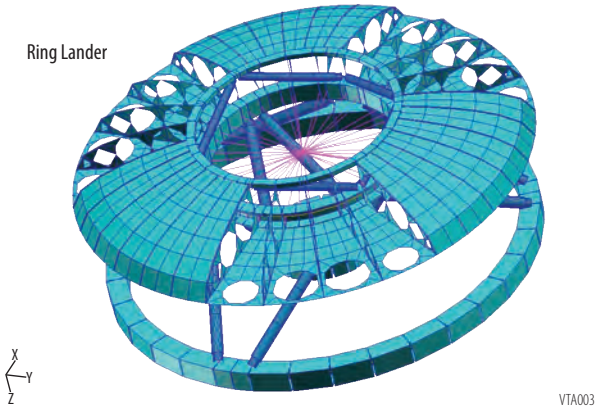


Figure 16: Ring lander finite element model

Table 10 shows how the design meets the analysis goals. For the landing load analyses, the material properties and allowables used were degraded due to the Ovda Regio surface temperature.

The analysis efforts performed to date focused on the survivability of primary and major secondary structural components. Preliminary analyses show the lander design meets the gross load and stiffness goals. Future analyses of the pressure vessel and internal components, including the Laser (due to the tight alignment requirements), are required.

3.2.4.3 Lander Mechanisms

Each VITaL mechanism (**Figure 17**) comprises a basic mechanical design with extensive flight heritage (TRL 6). The position resolutions, listed in **Table 11**, represent easily attainable target values for these types of mechanisms. All drive mechanisms comprise a stepper motor coupled to an appropriately-sized planetary gear set (**Table 11**). A separate mechanisms control electronics box (shown in **Figure 14**) is required to control the actuators.

Table 10: Analysis Results

Design Goal	Requirement	Ring
Fund. Freq (in aeroshell)	> 35 Hz	35.2 Hz
Atmospheric Entry Load	Stress Margin of Safety > 0	Min. MS= 0.11
Level Landing Load	Stress Margin of Safety > 0	Min. MS= 0.25
Non-level landing load	Stress Margin of Safety > 0	Min. MS= 0.71

Table 11: VITaL Mechanisms

	Panoramic camera	Filter Wheel	Raman/ LIBS focus	Raman/LIBS pointing
Positional resolution	N/A	N/A	5 µm	1.6 mm @ 2.5 meters
Range of motion	0 - 270°	0 - 300°	+/- 5mm	0 - 20°
Output drive mechanism	Spur gear	Spur gear	Lead screw	Spur gear
Positional feedback device	Switch or Encoder	Switch or Encoder	Encoder	Encoder

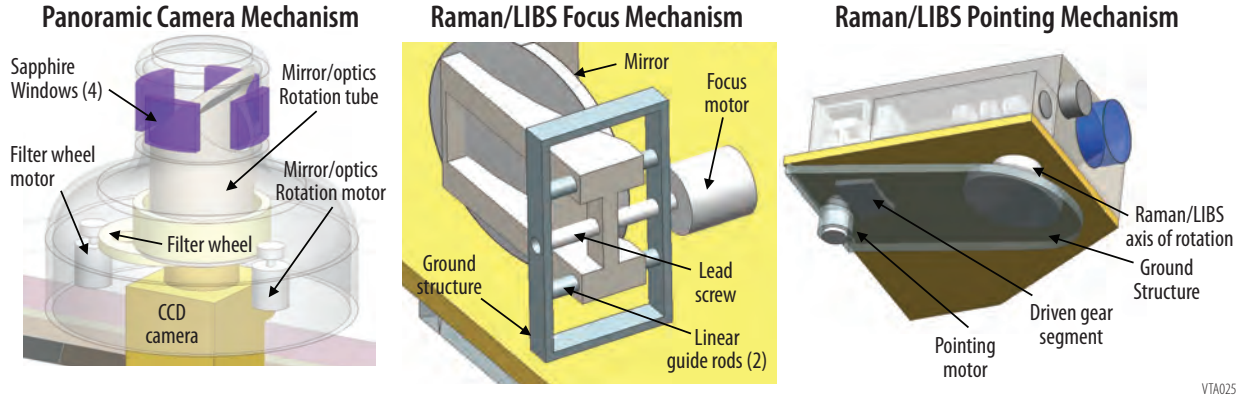


Figure 17: Mechanisms for A) Panoramic camera and filter wheel, B) Raman/LIBS focusing, and C) Raman/LIBS and Context camera pointing

3.2.4.4 Lander Thermal

The Venus atmosphere presents a unique thermal environment. The temperature of the atmosphere is 447° C, with a pressure of approximately 81 bar at the surface in the Ovda Regio (approximately 2 km above mean planetary radius). The three-hour mission life includes a one-hour descent through the atmosphere, and 2 hours spent on the Venus surface. The operational temperature limits of the avionics and instruments are assumed to be -20° C to 40° C, and their total heat dissipation is expected to be 239 W on the surface. The interior of the lander is pressurized at 1 bar, and natural convection is assumed to take place inside the pressure vessel.

The thermal strategy for this design concentrates the cooling directly at the electronics, and thermally isolates the two electronics decks from the rest of the lander. Phase change material (PCM) is embedded inside the decks to provide maximum conduction to the electronics, which are mounted on top of the decks. Lithium nitrate trihydrate (LNT) is selected as the PCM. LNT was flown on the Russian Venera landers, and minimizes mass and volume. **Figure 18** shows a graph of temperatures during the three-hour mission.

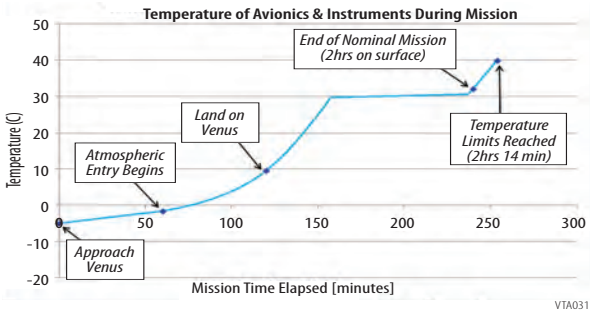


Figure 18: Lander Temp During Mission

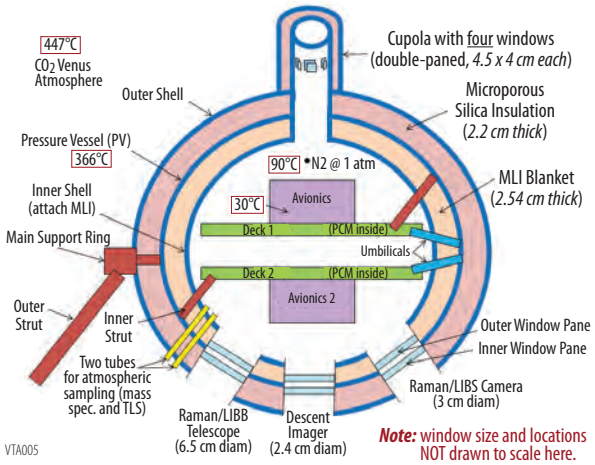


Figure 19: Thermal sketch of lander

The outer layers of the thermal protection system, as shown in **Figure 19**, include a layer of microporous silica insulation (2.2 cm thick), followed by a 40-layer Multi-Layer Insulation (MLI) blanket. Microporous silica was selected for its high temperature tolerance (up to 1000° C) and low thermal conductivity (0.035 W/mK). The MLI blanket design is similar to that used on the Pioneer Venus large probe.

There are multiple heat leaks into the pressure vessel, as quantified in **Figure 20**. Seven sapphire windows are required for conducting science observations from within the lander. Each window is double-paned, with a small air gap between for thermal insulation. There are two small intake tubes for NMS and TLS to collect atmospheric gas samples during descent. An umbilical runs from the outside of the lander, through the insulation, and connects to the carrier, contributing additional heat input. To increase thermal isolation of the decks, the internal support structure is designed using flexures with small cross-sectional area to minimize the heat flow from the pressure vessel wall to the decks.

The Systems Improved Numerical Differencing Analyzer (SINDA) analysis performed for this model assumes the heat is spread evenly over the deck. In later iterations of the design, it may be necessary to compensate for possible hot spots on the deck; if this occurs, the aluminum deck plate could be made thicker, to spread the heat more evenly, and/or additional heat spreading devices may be used. It may also be necessary to place an amount of PCM locally at the cameras, which are close to the high-temperature windows. Model predictions currently show that 50 kg of PCM (13 kg of which is packaging) are needed to keep the electronics at or below 35° C for the duration of the three-hour science mission (**Figure 18**).

3.2.4.5 Lander Optics

VITaL includes four optical instruments: Descent camera, Panoramic camera, Raman/LIBS context imager, and Raman/LIBS spectrometer.

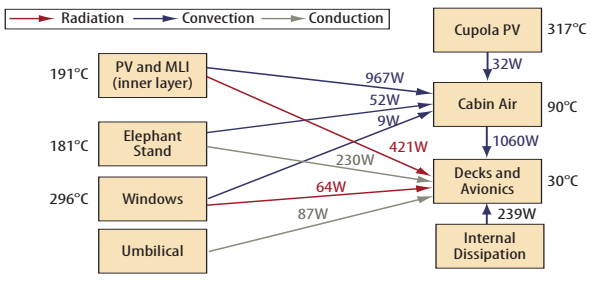


Figure 20: Diagram of heat leaks

Descent IR Camera

The Descent Camera (**Table 12**) images the Venus surface during descent. The 1.0 µm wavelength minimizes scattering at shorter wavelengths and absorption at longer wavelengths [Crisp, 2000]. The instrument aperture diameter is 8 mm (the window is 24 mm). The aperture is set at the back surface of the sapphire window to minimize thermal window size (**Figure 21**). Optical components are minimized to reduce mass while still maintaining image quality and the RMS spot size within one pixel across the full FOV.

Panoramic Camera

The Panoramic Camera (**Table 13**): 1) surveys the local terrain, and 2) provides context imaging for the narrow focused Raman/LIBS context camera. The Panoramic camera covers a FOV from 25° below to 10° above the lander's horizon, and ±30° in azimuth (**Figure 22**). During the mission, a mirror is rotated to four azimuth angles (0°, 90°, 180°, and 270°) about the lens axis. The panoramic camera takes images at λ = 550, 650, 750, 850, 1000 nm, with a bandwidth Full Width Half Maximum (FWHM) of 20-30 nm. It also takes an image with a clear aperture, using the CCD's natural responsivity curve. Because the intensity of the beam from a clear aperture is much higher than that passed through bandpass filters, a neutral density filter is added to get the intensity to the same order of magnitude. The defocus blur at 2.5 m is less than a pixel.

Table 12: Descent Camera Specifications

FOV	±20°
Spatial resolution	0.04°
Wavelength	1.0µm with 20nm bandwidth
S/N	>100 with 1ms exposure time
Detector	1024×1024 with 13µm pixel size
Size	5cm×5cm×7.5cm (exclude window and detector)
Mass	~100g (lenses only)
Exposure time	1ms

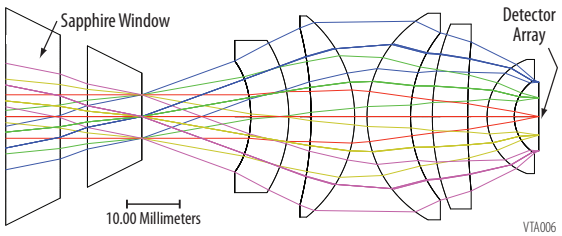


Figure 21: Descent Camera Optics

Table 13: Panoramic Camera Specifications

FOV	35° in elevation and 60° in azimuth (both full FOV)
Spatial resolution	0.25cm at 2.5m
Wavelength	550nm – 1000nm
S/N	>1500 with 100ms exposure time
Detector	2k×2k with 8.5µm pixel size (1338×2048 pixels imaged)
Instrument Size	5cm×5cm×11cm (lenses and mirror only)
Mass	~150g (lenses and mirror only)

Raman/LIBS Context Imager

The Raman/LIBS Context Imager (**Table 14**) is designed to monitor the laser spot position with respect to the scene using a single 550-700 nm filter. To minimize data volume, the laser spot (250 µm) is slightly under sampled (2.48 versus 3 pixels/laser spot) by the Context Imager. The wavelength range for this imager is limited to the CCD's spectral response, and the 532 nm laser spot may locally saturate CCD pixels. Even though the 532 nm laser spot is weaker than the 1064 nm laser spot, it is still strong versus the background noise. Camera optics are shown in the Appendix.

Raman/LIBS Spectrometer

The Raman/LIBS spectrometer (**Table 15**) is used for *in situ* mineralogy and elemental measurements. A Q-switch pulse laser with dual wave-

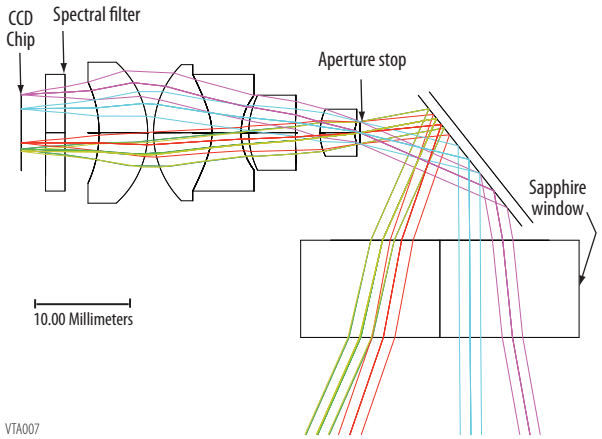


Figure 22: Panoramic Camera Optics

Table 14: Raman/LIBS Context Imager Specifications.

FOV	20cm×20cm
Spatial resolution	0.1mm
Wavelength	550nm – 700nm
S/N	>2500 with 30ms exposure time
Detector	2k×2k with 8.5µm pixel size
Size	5cm×5cm×20cm (lenses only)
Mass	~130g (lenses only)

Table 15: Raman/LIBS Spectrometer Specifications

FOV	±0.0033°
Spectral resolution	>2500
Wavelength	530nm – 700nm
Detector	3000×96 with 10µm pixel size
Size	26cm×21cm×10cm

length output (532 nm and 1064 nm) is used as the source to stimulate Raman and LIBS scattering. The same optics is used to focus the laser source to the target and to image the target on the slit (**Figure 23**). This implies that the slit and the laser source need to be co-aligned very well. The advantage of using the same optics is that the tolerance of the primary mirror and its mechanism is relaxed significantly due to the common path.

The FOV of the spectrometer is very small, which can be considered as a point source. The primary mirror (off-axis ellipse) longitudinal position needs to be adjustable due to object distance uncertainty. The large object to image distance ratio is critical for reducing adjustment range ($\Delta d_{obj} = \Delta d_{img} \times (d_{obj}/d_{img})^2$). Therefore, a single off-axis ellipse is selected as the telescope focus optic, which only needs to be moved ±5 mm for the expected distance variation of 2-3 m. The aperture size is scaled from Wiens et al.[2005], where the telescope aperture is 127 mm, and the target distance is 8.3 m. In the VITaL configuration, the distance is 2-3 m, thus the aperture is scaled to 65 mm and the laser source is kept at the same level.

The spectral range is 530 nm to 700 nm to cover both Raman and LIBS scattering. The spectral resolution is better than 2500 at the shortest wavelength and assumes the pixel size of the detector array is 10 µm.

3.2.4.6 Lander Avionics

Lander command and data handling (C&DH) is responsible for receiving commands from the flyby spacecraft, generating lander housekeeping data, integrating and buffering instrument data, providing the data to the RF system, executing the autonomous sequence of activities, and controlling the lander deployments.

Because the VITaL mission duration is short, the C&DH is single string. The mass is 7.9 kg, and the size is 17.5 x 9.0 x 10.5 cm. The power usage is 12.5 W from one hour before atmospheric entry through the end of the mission. During the coast phase between separation and one hour before atmospheric entry, the C&DH performs power strobing to reduce the required power to 1.65 W, after which it operates full on.

The C&DH block diagram is shown in **Figure 24**. The single board computer (SBC) provides command, control, and data handling. The ColdFire class processor is capable of handling the computational load. Memory/data storage requirements are minimal.

The SBC uses a SpaceWire RMAP (Remote Memory Access Protocol) interface and communicates to the other C&DH components using an on-board router. The Communications Driver card applies convolutional encoding and Reed-Solomon encoding to the data sent to the flyby spacecraft and for receiving commands. Two identical analog to digital converter boards process the thermistors and magnetometer data. Two cards are required because each analog interface requires two wires and 32 such interfaces would require 107 mm of card edge. Another 37 mm of card edge are required for the SpaceWire connectors. The Deployment Card controls the Lander aeroshell and instrument pyros (instrument mechanisms are controlled in a separate box). Actuation of any deployable requires two

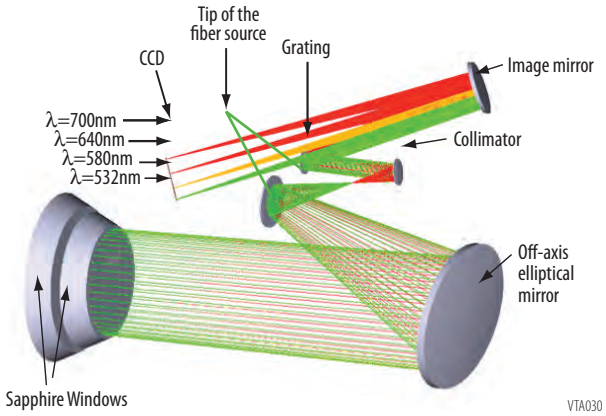


Figure 23: Spectrometer Optics

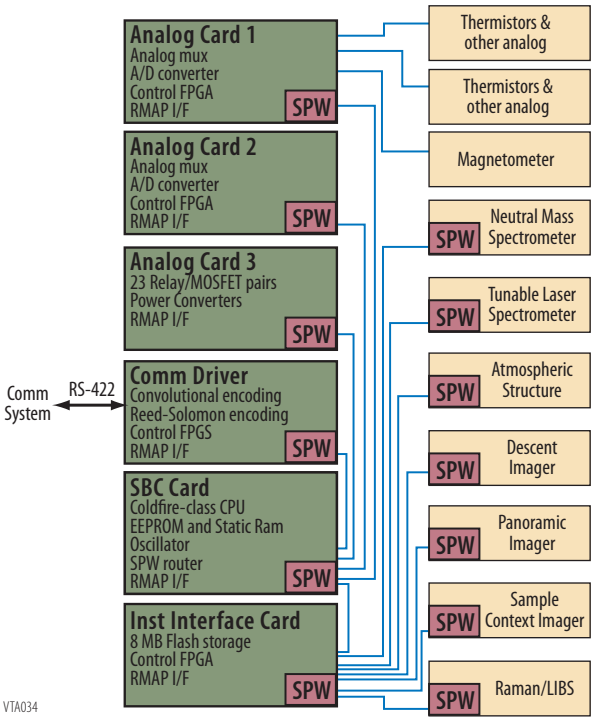


Figure 24: Lander C&DH block diagram

commands: arm and fire. There are 23 pairs of relays and MOSFETS for controlling the lander. The Instrument Interface card provides the interface and data storage.

The lander C&DH requires no new technology or novel designs. While the specific components in the current design may no longer be available in 2016 (beginning of Phase B), they are expected to be replaced by components that provide greater capability at lower power.

3.2.4.7 Lander Communications

The VITaL mission duration, from entry to end-of-mission, lasts approximately three hours. During that time, data is collected at variable rates to maximize performance and transmission. An S-band communication link is baselined, since the Venus atmospheric attenuation from the surface is small compared to other frequency bands (less than 3 db for elevation angles above 10°). The communication system aboard the probe is designed to maximize data transmission throughout the full mission duration. The system takes into consideration the flight trajectory and the changing uplinked science data quantity, depending on the angle of the landing site versus the carrier spacecraft. The system also allows for delayed uplink to the carrier spacecraft in the case of local topography blockages. The VITaL probe communications system consists of an S-band transponder, which allows commanding and two-way Doppler, as well as a 50 W Traveling Wave Tube Amplifier (TWTA) and supporting radio frequency (RF) components for uplink/downlink capabilities, as shown in **Figure 25**.

The communications system can be commanded to support telemetry data rates from 8.5 to 200 kbps. Telemetry is BPSK-modulated and convolutional (rate-½) and Reed-Solomon (255,223) coded, which provides margins of 3 dB or better for bit-error-rate of 10^{-6} at all ranges and elevations, as shown in **Figure 26**.

Subsystem components are commercial off the shelf, except for the omnidirectional antenna, which needs to be redesigned to use materials appropriate for the Venus atmospheric composition and temperature. The TWTA needs to be redesigned for the required RF power output and mission operational frequency. The transponder output power needs to be modified to meet TWTA maximum input power.

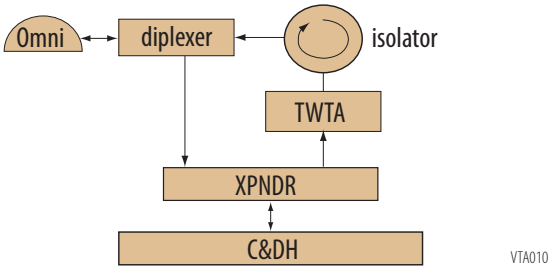


Figure 25: VITaL probe communication system block diagram

3.2.4.8 Lander Power

The lander power supply is provided by 100 SAFT LSH-20 Lithium-Thionyl Chloride primary cells. Primary batteries cannot be re-charged once discharged. Once the batteries are installed, the lander must be powered externally through an umbilical during I&T and the cruise phase of the mission. The battery package has 10 kg of battery mass and requires 2 kg of packaging. The cells have a capacity of 4413 Watt-hours. The batteries are assumed to lose 6% capacity corresponding to two years before use, and reach a depth of discharge (DOD) of 64% at the completion of the landed mission. The lander batteries reach a DOD of about 40% during the 5-day cruise after probe release and before reaching the Venus atmosphere. This is as a result of 5 day x 15 W for survival heaters/power strobing avionics. This estimate includes the probe's daily communication passes to the carrier spacecraft. The battery supplies power at two voltages: 31 V and 3.3 V (to save on DC/DC converter losses).

3.2.4.9 Lander Mass and Data Rate

The overall launch mass is shown in **Table 16**. Within the pressure vessel, the structure and the thermal design are the primary subsystem drivers. The large ring mass below the pressure vessel mass lowers the center of gravity. Mass margin of 22% still exists for the mission, even after applying 30% mass growth allowance to the current best esti-

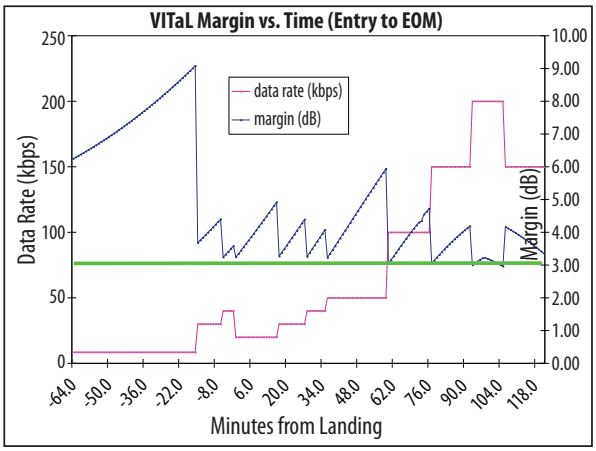


Figure 26: VITaL link margin with 40º incline versus data rate

Table 16: Overall Launch Mass with Probe Details

Item	CBE (kg)	Composite Mass Growth Allow. (%)	Max Expected Mass (kg)
Probe (Lander + Aeroshell)	2102	30%	2745
Lander	1051	30%	1366
Lander Science Payload	48	30%	63
Lander Subsystems	1002	30%	1303
Mechanical/ Structure	283	30%	368
Landing System	603	30%	784
Thermal	67	30%	87
Power	12	30%	16
Harness	10	30%	13
Avionics	8	30%	10
Mechanism Control Electronics	10	30%	13
RF Comm	9	30%	12
Aeroshell	1051	30%	1379
Heat Shield	718	30%	933
Backshell	293	30%	394
Parachute System	40	30%	52
Spacecraft	846		1100
Satellite (S/C + Probe) Dry Mass	2948		3845
Propellant Mass (3σ)	351	1%	355
Satellite Wet Mass	3299		4200
LV Throw Mass available to lift Wet			5141
Mass Margins			
LV Limited Max Wet Mass [kg]			5141
Propellant in LV Limited Max [kg]	430	3%	443
LV Limited Max Dry Mass [kg]			4698
Project Margin (Wet Mass Growth, MEV to LV Limit) [kg]			941
Wet Mass Growth (Wet Mass Growth, MEV to LV Limit) [%]			22%
Total Possible CBE Dry Mass Growth			860
Total Possible CBE Dry Mass Growth [%]			29.2%

mates for the 2021 launch window. **Table 17** provides details of power usage and battery sizing. During the 5-day coast from the carrier spacecraft to the Venus atmosphere, 15 W is assumed for communications, avionics, and positive thermal control to ensure the probe encounters the Venus atmosphere at approximately -5° C. The communication system is turned on only to broadcast for brief periods daily. The Probe Data Rate up to the carrier spacecraft is detailed in **Section 3.2.1**.

3.3 Ground Systems

The ground data system is shown in Figure 27. VITaL uses an X-band downlink to a DSN 34-meter ground station for both science data relay (through the 1 m HGA) and full duplex contingency communications (through two omni-directional antennas). X-band was selected instead of Ka-band because the carrier spacecraft requires contingency communications and Ka-band omni-directional antennas are not currently

Table 17: Overall Probe Power versus Battery capacity.

Max. Exp. Value (CBE + 30%)	Probe Cruise	1 hour before descent	Probe Descent	Probe Science	Probe Comm
Probe Power	15	166	272	239	156
Probe Watt-hours	1773	166	295	460	5
Lander Average during Duration	15	166	272	239	156
Lander Science Payload	0	0	83	63	0
Mass Spec	0	0	50	5	0
TLS	0	0	16.8	1.7	0
Atmospheric Package (Temp, Press, Magnmtr, etc.)	0	0	3.2	0.3	0
Magnetometer	0	0	1	0.1	0
Near Descent IR Camera	0	0	12	0	0
Panoramic Camera	0	0	0	3	0
Raman/LIBS Camera	0	0	0	3	0
Raman/LIBS	0	0	0	50	0
Total time of use (minutes)	7200	60	71	118	2
Duration of Period (hours)	120.0	1.0	1.1	~2.0	~0.0
Lander Subsystems	15	166	166	176	156
Mechanical / Structure	0	0	0	0	0
Thermal	12	0	0	0	0
Mechanism Electronics	0	10	10	20	0
Power	0	12	12	12	12
Harness	0	2	2	2	2
Avionics	2	13	13	13	13
Watt-hour total					**2699**
Battery capacity after 2 years					**4217**
Depth of Discharge					**64%**

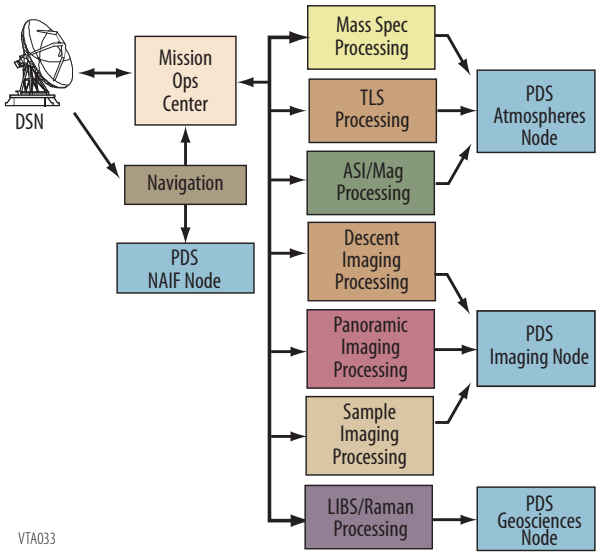


Figure 27: Ground system diagram

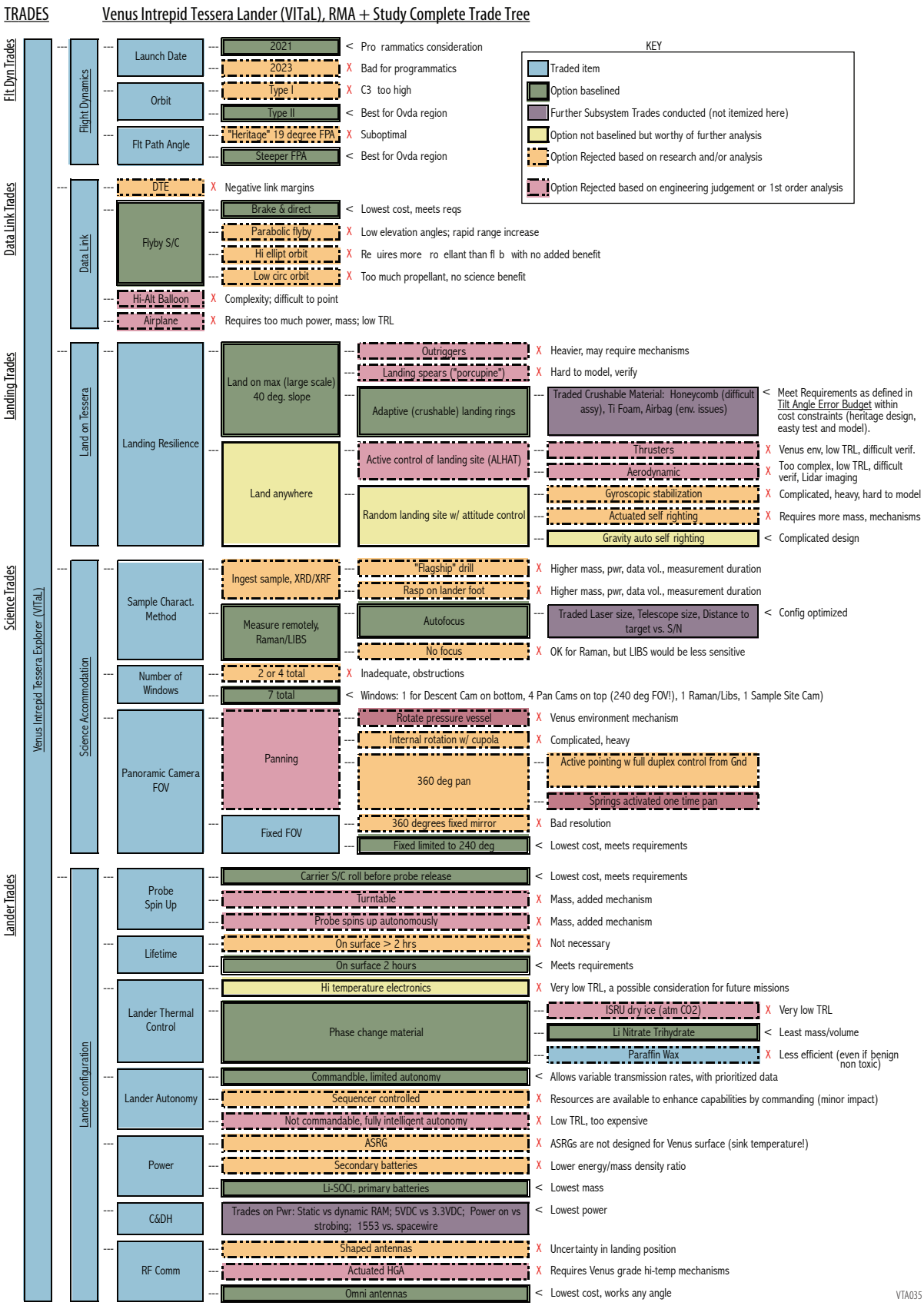


Figure 28: VITaL trade tree

available. The lack of Ka-band omni-directional antennas, and the low volume of science data (less than 1 Gbit), does not require the performance of Ka-band, resulting in lower cost and mass. If Ka-band is mandated for all science data downlink, VITaL could implement it with a modest increase in the cost and complexity of the carrier spacecraft communications system.

VITaL does not require the use of the 70-meter antennas and uses only one ground station at a time, with the exception of infrequent Delta Doppler One-way Ranging support to refine the navigation. The Navigation function is responsible for determining the trajectory of the spacecraft, planning maneuvers, and supporting lander release.

The Mission Operations Center (MOC) is responsible for carrier spacecraft operations and monitoring autonomous lander operations. During lander operations, the carrier spacecraft receives telemetry data from the lander via the S-band High Gain Antenna, and relays low rate status data to Earth using an X-band omni-directional antenna. The one-way light time to Earth is about 12 minutes. After lander operations have ended, the carrier spacecraft points the 1-meter X-band HGA to Earth and sends the data at 25 kbps. The total science data volume is between 356 Mbits and 964 Mbits. Once the data is reliably returned to Earth, the VITaL mission ends – about 9 months after launch.

The instrument teams process the science data and deliver the science data products to the Planetary Data System within 6 months of the end of mission operations.

3.4 Key Trades

For the VITaL study, more emphasis was placed on in-depth "real" engineering in selected areas of interest than would have been in a typical rapid mission architecture study. Accordingly, in addition to the usual mission and system level trades completed (orbit and flight dynamics, landing site selection, science requirements and instrumentation, mission lifetime and thermal architecture, power source, degree of lander autonomy, communication architecture, and operations), a significant number of trades for VITaL were also performed at the lower subsystem and discipline levels (**Figure 28**). The most extensive subsystem trades were associated with the landing subsystem architecture, using resilience versus communications and instrument performance as the figures of merit. The viable candidate options were then further refined by trades within the following disciplines:

A. Mechanical design: Concepts were ranked using the results of Finite Element analyses as the primary figure of merit. Lower level trades conducted to optimize critical components, such as the crushable material (metal foam) used in the landing rings.
B. Optics: Trading refractive vs. reflective; windows layout, size, and material; focusing approach. The optics trades were supported by FOV, geometric optics, signal to noise, and ray trace analyses as required, providing the figures of merit.
C. Avionics: Trades on operating voltage, data network architecture, and power strobing were made using power consumption and computing performance as figures of merit.

3.4.1 Lander Design Trade

The Cage Lander, developed as an alternative to the Ring Lander, has a rotatable pressure vessel protected on all sides by structure (**Figure 29**). This design has the advantage of operating even if it flips upside down. However, because structural members (the cage) fully envelope the pressure vessel and because the pressure vessel will rotate within the cage, panoramic camera, omni antenna, and Raman/LIBS instrument FOVs are potentially affected. Measures may be taken to ensure adequate science can be returned (e.g., adding actuators to move the cage structure, post-landing, away from the "up" side of the lander to ensure adequate instrument and omni FOVs).

Dynamically, the cage design need not fully absorb the impact energy because there is no lost

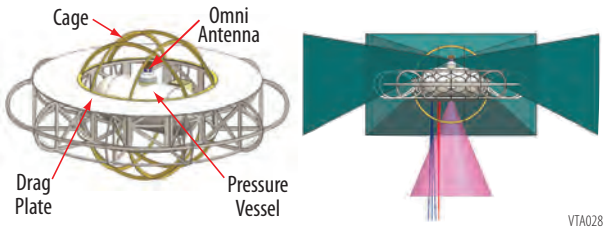


Figure 29: Cage Lander design A, without crushable material, A) Iso view; B) Instrument FOV

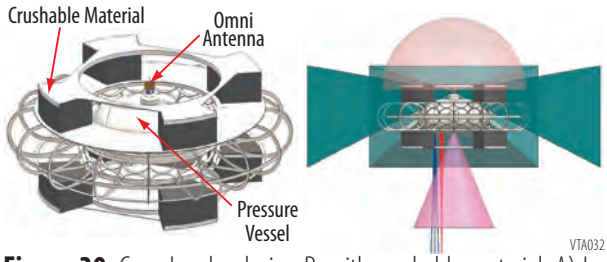


Figure 30: Cage Lander design B, with crushable material, A) Iso view; B) Instrument FOV

capability if it bounces and flips. This allows for a less rigid structural design that may include some amount of crushable material. A second version of the cage design has been generated that has an annulus region of crushable material above and below the pressure vessel (**Figure 30**). Using crushable material rather than the cage to protect the pressure vessel enables the omni antenna to function without the heavy communication uplink penalty of the cage (which acts as a reflector for the long wavelength S-Band). **Figure 29b** and **Figure 30b** illustrate the instruments' FOV for each cage lander concept, although further study is needed to fully compare each cage design. Both cage designs take advantage of the pressure vessel's ability to rotate to an "omni-up" pose within the cage. This controlled rotation is accomplished by incorporating a motorized rotating counterweight within the pressure vessel that will alter the vessel's center of gravity, causing the pressure vessel to rotate. Both cage landers also have the advantage of being lighter than the Ring Lander, possibly allowing a smaller launch vehicle. **Table 18** provides an assessment of the two alternative cage designs versus the baseline Ring Lander. The Ring Lander was chosen as a baseline due to its lower complexity and cost, but there are advantages to the other designs. A figure of merit value of 5 is essentially high performance and off-the-shelf, while a 1 means that characteristic is a significant risk or requires major development.

Table 18: Lander trade matrix

	Ring Design	Cage Design A	Cage Design B
Estimated mass (kg)	1200	580	750
Complexity - Analysis	4	2	3
Complexity - Assembly	4	3	3
Complexity - Design	4	2	3
Complexity - Fabrication	4	4	4
Complexity - Mechanisms	5	5	5
Flipping Avoidance	4	2	3
Flipping Survivability	1	4	4
Drop Testing/Environmental	4	2	3
Testing Validation	4	2	2-3
Omni FOV	4	2	3
Panoramic FOV	4	3	3
Raman/LIBS FOV	3	3	2
Pressure Vessel Protection	4	5	3
Cost	4	2	3

1 = large development effort, significant risk
2 = meets a few expectations, substantial development and some risk
3 = meets some expectations, significant development
4 = meets most expectations, some development
5 = meets all expectations, essentially off the shelf

3.4.2 Crushable Material Trade

Crushable material is required to enable the lander to "stick" the landing (not bounce). If the lander bounces, it may tip the lander over, even on a static stable landing site that would have been safe. Using crushable material reduces the g load on the lander at impact by plastically deforming or "crushing" to absorb the kinetic energy of landing. Crushable material can be foam, honeycomb, or custom structural shape. Most balloon-like materials (such as air bags used for landings on other planets) would either present a complex qualification challenge or will not survive in the Venus atmosphere. Propulsion systems are not easily achieved due to Venus surface temperatures and pressures.

Ideal crushable materials have: 1) a high void fraction (so the usable crushable stroke is maximized), 2) properties that don't degrade at Venus surface pressure and temperature, 3) isotropic properties (in case of side impacts), 4) near linear crushing under a constant pressure, and 5) predictable analytical and empirical performance. The Venera Landers had a hollow toroidal crush pad and shock absorbers for landing. Detailed description of this system is not provided in the available literature. This approach is analytically complex and difficult to build and test. The Venus Flagship Mission Report [Bullock, 2009] suggested the crushable material would be honeycomb. This works well only in some impact directions. The baseline Ring Lander uses a commercially-available high void fraction titanium foam material that has the advantage of being isotropic and open cell construction, which makes it pressure insensitive. Further studies need to be performed to develop a lander concept that would trade these materials.

3.4.3 Hazard Avoidance System Trade

The VITaL mission concept involves landing within a relatively hazardous region of the Venus surface with potentially high landing slopes and rough surface terrain. Including some form of active terminal descent trajectory control into the VITaL lander design would improve the probability of safe landing and mission success. This terminal descent system would require an autonomous hazard and terrain slope navigation system as well as some means to actively divert the lander's trajectory. Terminal descent systems that include this type of active hazard avoidance have been proposed for Mars and lunar landers. (Such systems are typically descoped due to cost.) Systems typically utilize radar or lidar for hazard detection and execute the trajectory divert through a descent

propulsion system. The Venus atmosphere, being quite different from Mars, likely requires different technologies to achieve the required navigation and control. Although implementation of hazard avoidance was considered too costly for VITaL, some potential concepts are described.

One such hazard avoidance design does not carry propulsive descent engines; instead, it relies on drag from the dense Venus atmosphere. Significant horizontal acceleration on the order of ~1.3 m/s^2 for a 1 m^2 reference area could be created using relatively small aerodynamic lifting surfaces. Among the options are: 1) moving aerodynamic fins, 2) fixed aerodynamic fins for lift force and moving control surfaces to effect equilibrium angle-of-attack/bank angle, or 3) fixed aerodynamic fins for lift force and some form of lander-internal momentum exchange devices (i.e., reaction wheels or control moment gyroscopes) to control bank angle and/or angle-of-attack.

This system still requires a navigation system for hazard detection and terrain slope identification over the feasible landing area during the terminal descent phase. Other studies have determined that, at altitudes less than 15 km, the properties of the atmosphere are conducive to utilizing near-infrared (NIR) systems to image the surface with enough resolution to detect hazards and local slope conditions as the vehicle approaches the surface. Surface images could be collected and analyzed autonomously to select feasible landing sites within the local terrain. On Venus, this may be difficult since the ambient light is highly reflected, and therefore, shadows are more difficult to perceive.

In-depth trade studies would be required to determine the best approach to hazard sensing (near infrared vs. radar vs. lidar) and aerodynamic navigation (fins vs. control surfaces vs. momentum exchange devices). The very low TRLs of such Venus grade systems and their complexities, coupled with the formidable difficulties of ground verification, all but guarantee that developing such systems aren't realistic under a single mission's New Frontiers cost cap.

3.4.4 Communications with Steeper Slopes

At landing, the carrier spacecraft is at approximately 40° elevation (elevation increasing) or approximately 50° from lander zenith. Approximately 73 minutes after landing, the carrier spacecraft passes roughly directly over the lander. Approximately 120 minutes after landing, the carrier spacecraft is at approximately 40° elevation relative to the lander (elevation decreasing). The omni antenna views the hemisphere directly above the lander, and can communicate with the carrier spacecraft only when it is unobstructed by the surrounding terrain. Therefore, if the terrain comes into the FOV between the carrier and lander, communications will be lost. This limits the angle that the lander can reach for this carrier trajectory. For the Cage Lander, communications are a particular issue, defined by interferences with the drag plate. Rotating the omni still does not enable more than a hemisphere above the lander. Additional omni antennas could be located for the Cage Lander, but this would require the omni signal wire to traverse the single axis rotation and still would not enable clear FOV if the local topography came into the FOV.

Landing slopes >40° impact full 2 hour communication viewing of the carrier spacecraft. A trade was done that looked at enabling complete communication coverage on a 70° slope for the full 2 hours after landing. This means the carrier traverses only ±20° from directly overhead. The downside is that the carrier spacecraft periapsis radius is increased to approximately 62,000 km, which increases the carrier spacecraft to lander range and effectively cuts the data rate by a factor of 5.4. The RF power limitation is a function of the heat sink ability of the TWTA. The large landing slopes disable many basic two-phase solutions traditionally used to cool high heat flux TWTAs. This concept could likely handle a TWTA with double the RF power, which could compensate for some of the greater range, but after that point, accommodation of the larger TWTA will become difficult. Therefore, it is better to take the risk of a landing beyond 40° blocking part of the 2 hours of communication, versus a carrier flight path that maintains constant communication but at a much larger range.

Table 19 shows the effect of landing angle on communications uplink totals. The angle assumes a worst case inclination (i.e., the inclination is within the plane of the lander and where the carrier is at landing and after 2 hours). If it is not in this plane, the impact could be lessened.

3.4.5 Other Trades

While some aspects of VITaL are highly unique, some (such as the carrier spacecraft, the

Table 19: Landing Angle Versus Data Return

Landing Angle	Data Return (Mbits)	% of max
0°	964	100%
40°	723	75%
60°	356	37%
70°	248	26%

aeroshell, the RF communications architecture, etc.) are very similar, and in some cases identical, to those in the Venus Mobile Explorer (VME) study [2010] completed by the same ADL team for the same customer. After critical inquiry, it was established in a number of areas (such as the carrier spacecraft or the RF Communication architecture), that the conclusions of the VME trades still hold. In those areas, the results of the VME trades were adopted.

3.5 Risk List

The study team identified three significant VITaL development risks and three operational risks. Each risk is described in **Figure 31**.

Development Risks

1. Safe Landing Assurance: The lander is equipped with a robust landing system and has plenty of mass allocation, though the design needs considerable non-linear dynamic analysis and drop testing. Development of tessera-like landing scenarios for the drop tests and the inevitable design challenges will commence in the pre-Phase A portion of the mission, lowering this risk.
2. Test Facilities: The "test as you fly" philosophy is challenging for the VITaL probe due to the high temperature, high pressure, and unique venusian atmosphere. Facilities that could be used to simulate Venus entry conditions and Venus surface conditions are not designed to accommodate large test samples. Also, the mission has a two hour lifetime (or less in the case of the aeroshell) and the hardware is irreversibly damaged at the end of its mission; that cannot be tested on the ground. Verifying basic functionality in a near full scale facility remains crucial to keeping the mission risk within acceptable limits. However, some functionality needs to be separately qualified with flight-like components to prevent permanent damage to the flight article.

 For qualifying the aeroshell, several arcjet facilities for material testing currently exist in the US and around the world. However, there are limitations to achieving applicable conditions in ground test facilities for CP qualification. This is a potential risk, as heritage CP is the only material known to work for Venus entries. (See Venkatapathy et al., 2008; 2009 for additional information about qualification and risks associated with VITaL. Recommendations have been made to upgrade existing arcjet facilities to generate very high heat fluxes (7-8 kW/cm^2) as well as operate in CO_2.
3. Raman/LIBS Development: The baseline LIBS instrument needs additional development to reduce calibration and sizing complexities that introduce uncertainty into the measurements, particularly in the Venus environment. Completing demonstration tests in a relevant environment with a similar Laser and Telescope size lowers this risk. The lowest TRL element in the instrument is a 65 mJ laser that can survive the 200 g loads.

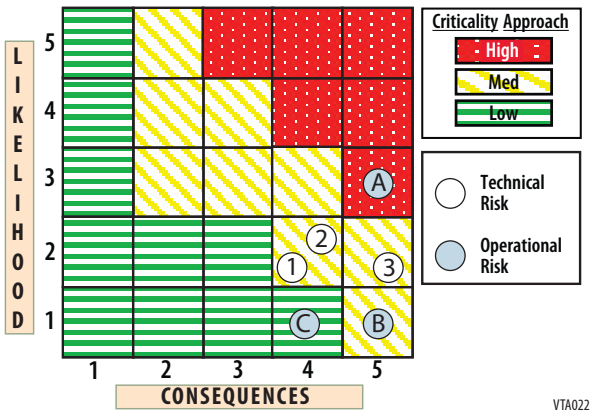


Figure 31: VITaL Risk Matrix

Operational Risks

A. Landing Risk: There is an inherent risk that the lander may flip due to unforeseen circumstance (e.g., a boulder or hole). This risk is residual throughout the mission. Missions flown before the VITaL launch could mitigate this risk by providing images and topography to help select the lowest risk landing ellipses.
B. Aeroshell Operations: Due to operations complexity and significant mechanical and thermal loads, the aeroshell may not perform as planned. This is a difficult "test as you fly" component and this risk is residual throughout the mission.
C. Raman/LIBS FOV does not see the surface: If the lander is tilted or lands on a peak, then the Raman/LIBS viewport may not view any surface rocks. The FOV tilts below the plane defined by the drag plates by 10°. If a rock tilts up the lander such that the Raman/LIBS does not view the surface, then the measurements of the surface could not be taken. This risk could be mitigated by additional resources.

3.6 Technology Maturity

The primary requirement for the VITaL design was to develop the most cost effective lander for

landing in a tessera region. To save on development, analysis, and testing costs, external mechanisms were considered too expensive to implement. Therefore, all mechanisms in the lander as well as the instrumentation are at a fairly high TRL level. The exception is the Raman/LIBS instrument. VITaL's Raman/LIBS has a significant two-stage Laser and a large telescope because it is being designed to take measurements 2.5 m away (enabling the 0.86 m survey line for a 20° mechanism swing) rather than directly underneath. The laser and optics are similar to other flight lasers and optics, but these have not been designed to survive 200 g. Sensitivity requirements for these instruments also need to be evaluated in depth.

Another open issue is how best to implement the large number of optical windows that all need to be hermetically sealed. This may require some science compromises or structural creativity.

The landing system requires some optimization, and brass board and engineering model testing, but in this concept, no new technologies are required. Finally, a study to evaluate the use of a primary battery versus a secondary battery is recommended. All of these technology maturation plans can be performed within a New Frontier's schedule, pending independent assessment/development of the state of the art of the Raman/LIBS system.

4.0 DEVELOPMENT SCHEDULE AND SCHEDULE CONSTRAINTS

4.1 High-Level Mission Schedule

Figure 32 provides a realistic high-level mission schedule. The schedule starts with lower TRL item development, resolving development work early before it becomes the critical path. Because of VITaL's high TRL approach for the baseline Ring Lander, early pre-phase A work can be completed in a New Frontiers baseline schedule. It is important to develop the landing requirements in a way that can be designed for, analyzed, and tested in a reasonable fashion. The decision as how best to implement the Raman/LIBS (see **Section 3.5**) and panoramic camera mechanical/optical design in the cupola also need to be resolved early. The mission, as outlined in this concept, does not represent a high development risk mission.

4.2 Technology Development Plan

The technology development plan requires technology development to start approximately 1 ½ years prior to SRR. This allows the Raman/LIBS, mechanical structure with windows, power, and landing system designs to be developed sufficiently that the system requirements can be derived and the other subsystem requirements can be baselined. This plan depends on a Venus

VITaL Project Schedule

ID	Task Name	Duration	Start	Finish
1	**Phase A: Concept & Technology Development**	**420 days**	**Mon 8/4/14**	**Fri 3/11/16**
2	Mission Design Concept / AO Development	6 mons	Mon 8/4/14	Fri 1/16/15
3	LIBS/Raman Development	12 mons	Mon 8/4/14	Fri 7/3/15
4	Venus Environmental Test Chamber complete	0 days	Tue 1/5/16	Tue 1/5/16
5	Landing Ring Design	12 mons	Mon 8/4/14	Fri 7/3/15
6	Comm Relay Design Concept Study	6 mons	Mon 1/19/15	Fri 7/3/15
7	Battery Study	6 mons	Mon 1/19/15	Fri 7/3/15
8	Instrument Announcement of Opportunity	6 mons	Mon 1/19/15	Fri 7/3/15
9	Instrument Selection	3 mons	Mon 7/6/15	Fri 9/25/15
10	Mission Requirements Development	6 mons	Mon 9/28/15	Fri 3/11/16
11	Mission Requirments Review	0 days	Fri 3/11/16	Fri 3/11/16
12	**Phase B: Preliminary Design & Technology Completion**	**380 days**	**Mon 3/14/16**	**Fri 8/25/17**
13	Systems and Subsystem Requirements Development	6 mons	Mon 3/14/16	Fri 8/26/16
14	System Requirements Review	0 days	Fri 8/26/16	Fri 8/26/16
15	Carrier S/C Preliminary Design Development	10 mons	Mon 8/29/16	Fri 6/2/17
16	Probe Preliminary Design Development	13 mons	Mon 8/29/16	Fri 8/25/17
17	Carrier S/C Preliminary Design Review	0 days	Fri 6/2/17	Fri 6/2/17
18	Probe Preliminary Design Review	0 days	Fri 8/25/17	Fri 8/25/17
19	**Phase C: Final Design and Fabrication**	**400 days**	**Mon 8/28/17**	**Fri 3/8/19**
20	Carrier S/C Subsystem Development	6 mons	Mon 8/28/17	Fri 2/9/18
21	Carrier S/C Critical Design Review	0 days	Fri 2/9/18	Fri 2/9/18
22	Carrier S/C Flight Hardware Fab & Test	12 mons	Mon 2/12/18	Fri 1/11/19
23	Probe Subsystem Development	8 mons	Mon 8/28/17	Fri 4/6/18
24	Probe Critical Design Review	0 days	Fri 4/6/18	Fri 4/6/18
25	Probe Flight Hardware Fab & Test	12 mons	Mon 4/9/18	Fri 3/8/19
26	**Phase D: System Assembly, Integration and Test, and Launch**	**685 days**	**Mon 3/11/19**	**Sat 10/23/21**
27	Carrier S/C System Level Integration & Test	6 mons	Mon 3/11/19	Fri 8/23/19
28	Carrier S/C Environmental Test	5 mons	Mon 8/26/19	Fri 1/10/20
29	Probe System Level Integration Test	6 mons	Mon 3/11/19	Fri 8/23/19
30	Probe Environmental Test	5 mons	Mon 8/26/19	Fri 1/10/20
31	Probe to Orbiter Integration & Test	4 mons	Mon 1/13/20	Fri 5/1/20
32	Spacecraft environmental testing	5 mons	Mon 5/4/20	Fri 9/18/20
33	Launch Site Campaign	5 mons	Mon 9/21/20	Fri 2/5/21
34	Mission Slack	9 mons	Mon 2/8/21	Fri 10/15/21
35	Launch Spacecraft	0 days	Sat 10/23/21	Sat 10/23/21
36	**Phase E: Operations and Sustainment**	**202 days**	**Mon 10/25/21**	**Tue 8/2/22**
37	Cruise phase	111 days	Mon 10/25/21	Mon 3/28/22
38	1st Venus Flyby	81 days	Tue 4/5/22	Tue 7/26/22
39	2nd Venus Flyby	5 days	Wed 7/27/22	Tue 8/2/22

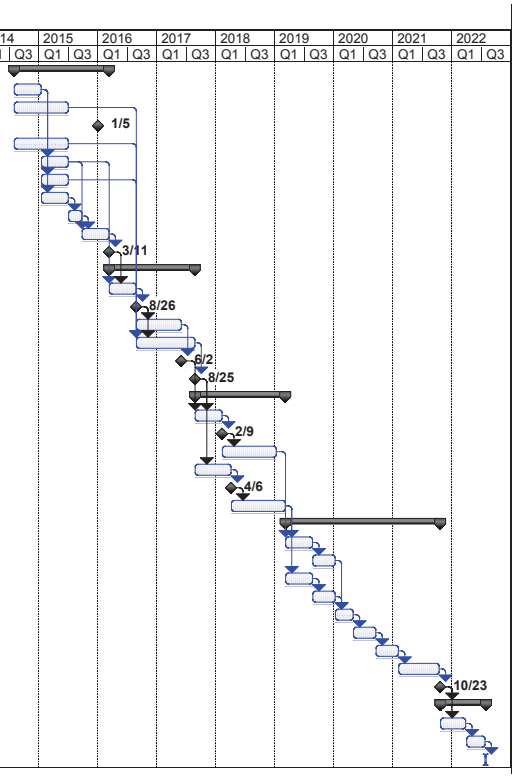


Figure 32: VITaL Overall Schedule

test chamber being developed for testing Raman/LIBS under Venus pressure, temperature, and in a CO_2 environment so the Raman/LIBS can be sized. The landing ellipse selection process would be enhanced by higher fidelity topography of Ovda Regio acquired before June 2019. This allows time for the lander to be targeted to a suitable region of Ovda that has a high likelihood of a landing location of greatest scientific interest. The current assessment of what is likely to be found in Ovda with macroscale slopes in the 30 to 40° range and lander scale roughness in the 0.5 to 1 m range suggest that the design as is, and Magellan scale topography, are sufficient to give a high confidence that landing could be successful.

5.0 MISSION LIFE-CYCLE COST

5.1 Costing Methodology and Basis of Estimate

VITaL costing methodology for the probe and carrier spacecraft is based on a combination of parametric cost modeling, analogies to prior missions, and historic cost wrap factors (to account for program support, mission operations, ground systems, etc.). Price H parametric model estimates are driven by preliminary Master Equipment Lists (MELs). MEL item masses, type of materials, TRLs, and complexity are combined with mission-level cost wrap factors to derive an initial estimated mission cost. A reserve of 50% on Phases A-D and 25% on Phase E is added to the total estimated mission cost, with the exception of the carrier spacecraft, where a 30% reserve is added. The 50% reserve equates to an approximate 70% confidence level in the cost certainty in conventional cost risk analysis. Because Venus surface missions are unique and there are no recent landed missions to provide engineering and development constraints, the parametric model cost certainty could be much lower than 70%. No reserve was added to the Launch Vehicle. All costs are in Fiscal Year (FY) 2015 dollars. No grassroots estimate was developed for the study.

5.2 Cost Estimate

Based on the Price H model and cost analogies during this study, the team estimated, at 70% confidence level, a VITaL mission concept total cost of $740M to $1.1B (without launch vehicle; $1.3B with launch vehicle). This cost range is at the high end of the New Frontiers cost limit (assumed to be $773M FY15, without launch vehicle) and into the low end of a flagship mission cost. This cost estimate uses an Atlas V 551. Based on the mass margins, an Atlas V 541 also is capable of launching this mission and a Atlas V 531 is within 39 kg of being capable. These choices were not available per the study ground rules. This might yield on the order of $20 million in savings. The New Frontiers cost limit is derived from the Planetary Decadal Survey statement of task and is $900 M (FY09 including launch vehicle) x 1.144 (to inflate to FY15) - $257 M for launch Option 5 from the study ground rules (~Atlas V 551). The major technology-development cost for this mission is the Raman/LIBS instrument development. The mission cost estimate includes $20M to bring new technology to TRL 6. There is also a rigorous development plan for the landing system, including brassboard and EM testing, and funding to support numerous drop tests as well as qualify the carbon phenolic process for the aeroshell. The Technology Development plan is provided in **Section 4.2**. Other cost risks were not analyzed in detail and were beyond the scope of this enhanced rapid mission architecture study.

For this mission to more-comfortably fit within a New Frontiers cost, the study team recommends focusing the mission on the three highest priority surface science objectives (**Table 1**). Removing the NMS, TLS, and Magnetometer not only reduces instrument cost but also reduces lander cost and program support costs. As the instrument mass and volume are reduced, the pressure vessel and thermal system sizing can be reduced. The associated system integration and test costs for those instruments also are reduced. A point design study to increase the cost confidence level is needed to provide a cost for this more focused mission.

6.0 CONCLUSIONS

The tessera regions of Venus provide fundamental clues to Venus's past, but the terrain has been viewed as largely inaccessible for landed science due to the known roughness. Studies of similar topography on Earth, the Moon, and Mars, however show that due to gravity forces, highlands-like regions typically have macro slopes of less than 30°. Stereo SAR Images from Magellan support this finding. Block sizes of similar regions are typically less than 1 m, suggesting the VITaL 1.3 m allowance is more than adequate.

This study report examined the possibility of landing in the highlands of Ovda Regio because its location near the equator ensures that a mission scenario could be found with excellent lighting conditions. Several possible landing ellipses were found that had average slopes on the km scale of less than 30° and do not contain intra-tessera plains. Extensive instrumentation is included in

the design concept to provide high fidelity context images along with extensive mineralogy and elemental measurements via a Raman/LIBS system. The Raman/LIBS system sizing was explored and a Raman/LIBS Laser and Receiver Telescope were sized. The system is smaller than some laboratory versions due to volume and power constraints, but there is a healthy amount of trade space open to optimize this system. There are trades yet to be performed, including a wider survey versus a more focused one, and high S/N surveys that need to be completed as the concept matures.

The Ring Lander can land on a block 1.3 m high that is sitting on a 30° slope without flipping or tumbling. This configuration was traded with alternate designs that had the ability to tumble. The complexity of those landers would have driven design, analysis, and testing costs beyond the New Frontiers budget goal. Mechanically surviving landing on steep slopes is not the only characteristic to consider when landing in the tessera. The data uplink to the carrier spacecraft also becomes an important driver for non-flat landings. For local slopes above 40°, part of the lander's ~2 hour lifetime at the landing site can be blocked by the surrounding terrain. Tolerating some blockage (which could occur at the beginning or end of the two hours) allowed more data return than altering the carrier spacecraft trajectory to a higher altitude and lowering the uplink rate (see **Table 19**). Therefore, the collected science data are prioritized on the lander before transmission to ensure the highest priority data reaches the carrier spacecraft. Landers with tumbling ability were less capable with uplink performance than the Ring Lander due to additional structure interfering with the antenna.

The VITaL mission concept has at least 22% mass margin (above the 30% mass growth allowance) if launched in 2021 on an Atlas V 551. The estimated cost is within the New Frontiers cost cap, adding the 50% growth allowance pushes it into lower end flagship range. Descopes that focus the mission on high priority surface science will result in a mission cost that better fits in the New Frontiers cost envelope.

7.0 OPEN TOPICS

1. Acquisition (through another Venus mission) of a topography map of Ovda, Alpha, Tellus, and Thetis tessera regions (with 1 to 2 m class imaging) would help to assess the best landing ellipse for mission success. Such a mission is not strictly necessary before flying VITaL, but it might enhance site selection.
2. Raman/LIBS sensitivity studies need to be performed in a Venus-like environment with the detailed optical and laser system detailed in this report to evaluate sensitivities. Likewise, testing in a Venus pressure and CO_2 environment needs to be performed. The g loading as a result of the entry angle may drive the laser design. If this turns out to be a major driver, further flight dynamics work needs to be performed to lower the entry angle.
3. Landing System Dynamics, including angular impacts, needs to be evaluated by drop testing prototype landers.
4. The complexity of accommodating large optical windows and interplay with structure and sealing needs to be evaluated. The cupola on top of the lander and the Raman/LIBS windows in particular should be engineered and tested on the early pressure vessel design.
5. The size of the Raman/LIBS aperture was driven by the size of the Raman/LIBS optics. Further studies should assess whether Raman/LIBS optics can be compacted to allow for a larger aperture window.
6. Flight Dynamics studies to examine additional trajectory options should be investigated, as well as finding a 2023 launch date that could land in a tessera region.
7. Additional structural analyses of internal components of the pressure vessel should be conducted.

ACKNOWLEDGEMENTS

NASA/GSFC Study Directors
- Martha Gilmore, VITaL Science Co-Champion
- Lori Glaze, VITaL Science Co-Champion
- Michael Adams, VITaL Study Lead
- Gabriel Karpati, Decadal Studies System Lead
- Michael Amato, GSFC Planetary and Lunar Lead

NASA/GSFC Systems Engineering
- Charles Baker, VITaL Systems Lead
- Joanne Baker, VITaL I&T Lead
- John Galloway, VITaL
- Steven Tompkins, VITaL Ops Lead

NASA/GSFC Engineering Team
- Ed Brinker, VITaL Avionics Lead
- Jeff Bolognese, VITaL Mechanical Analysis Lead
- Brent Bos, VITaL Optics
- Heather Bradshaw, VITaL Thermal Lead
- Phil Calhoun, VITaL Hazard Avoidance
- Matthew Garrison, VITaL Thermal Team
- Qian Gong, VITaL Optics Lead
- Andrew L. Jones, VITaL Structures Lead
- Greg Marr, VITaL Flight Dynamics Lead
- Tom Myrick, VITaL Mechanisms Lead
- Adan Rodrigues-Arroy, VITaL Communications Lead
- David Steinfeld, VITaL Thermal Team
- Timothy Stephenson, VITaL Materials Engineer

NASA/ARC Entry Descent Element (EDE) Team
- Ethiraj Venkatapathy, EDE Chief Technologist
- Helen Hwang, EDE Element Manager
- Gary Allen, EDE System Analyst
- Ken Hamm, Aeroshell Structural Analyst
- Bernie Laub, TPS Element Lead
- Todd White, EDE Engineer

NASA/GSFC Parametric Cost Team
- William Lawson, Parametric Cost Group Lead
- Sanjay Verma, Probe and Mission Parametric Cost lead

NASA/GSFC Report Development Group
- Steven Stuart, Report Development Specialist
- Ruth Jennings, Report Graphics Specialist

APPENDIX A – ADL PROCESS

Table A1: Using the ADL's five step process (see appendix), the study accomplished a systematic exploration, down-selection, and optimization, of the best architecture concepts for VITaL.

Step 1: Explore the trade space: expand, filter, and contract	The trade space was expanded to the maximum, then methodically narrowed and filtered through, yielding a list of potential architecture solutions.
Step 2: Build team per preliminary requirements	Conducted preliminary analyses of the candidate architectures. Consolidated team with the required expertise, finalized formal study partnership with Ames on aeroshell design.
Step 3: Finalize science payload	Compiled a straw-man science payload to serve as the anchor for the mission's minimum performance requirements.
Step 4: Conduct detailed analyses of viable architecture options	Conducted detailed architecture trades as described below
Step 5: Conducted assessment of architecture	Conducted assessment of architecture

APPENDIX B – ALTERNATIVE LANDING ELLIPSES

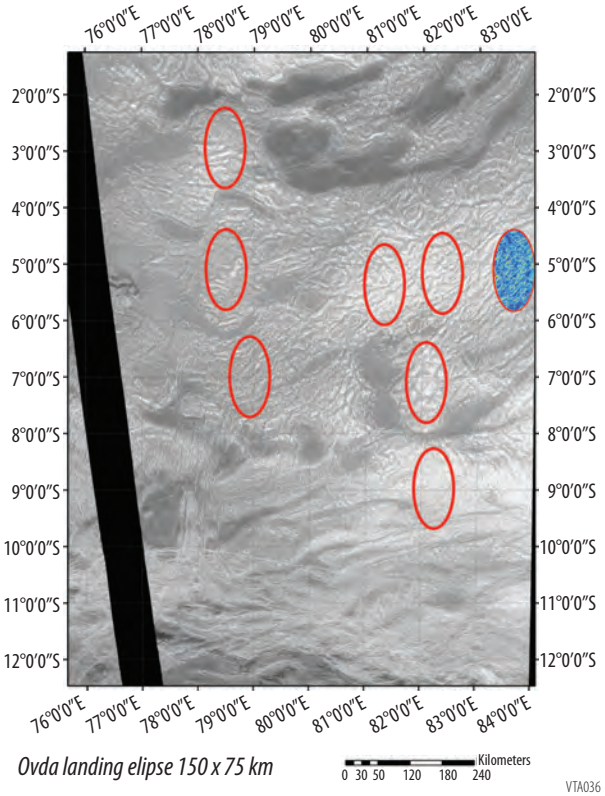


Figure B1: Sample VITaL ellipses within Ovda Regio. These ellipses are targeted to avoid intratessera plains and have moderate slopes <40°

APPENDIX C – DRAG PLATE SIZE VERSUS VELOCITY

Table C1 shows how the drag plate size (as a fraction of 3.2 meter disk which is the maximum that will fit in the aeroshell) affects the landing speed (by providing aerodynamic resistance in the Venusian atmosphere.) The landing system needs to absorb the kinetic energy of the lander with crush pads or it will bounce. The crush pad thickness is proportional to the square of the velocity, and linear with the mass of the lander.

Table C1: Table Drag Plate Size versus velocity

Mass of Lander (kg)	Fraction of Ø3.2m Drag plts	Terminal Vel (m/s)
1000	0.5	9
1100	0.5	9.5
1200	0.5	9.9
1300	0.5	10.3
1000	0.75	7.5
1100	0.75	7.9
1200	0.75	8.2
1300	0.75	8.5
1000	1	6.7
1100	1	7
1200	1	7.3
1300	1	7.6

APPENDIX D – AEROSHELL DETAILS

Table D1: Detailed heat shield and backshell mass estimates

	Zero Margin
Max Dia,m	3.5
BS structure	224
BS TPS	69
BS Total Mass, kg	293
HS structures	269
HS TPS (C-P)	449
HS Total Mass, kg	717
Parachute, kg	40
Total, kg	1050

Table D2: Un-margined and margined mass estimates

	Zero Margin	with 30% Margin
Aeroshell Mass	1050	1365
Payload mass, kg	1200	1560
Total Entry Mass,kg	2250	2925

Note: The carbon phenolic required for VITaL was slightly smaller than VME. Due to increased G'load from a limit load of 175'g for VME to 225 g' for VITaL, the structure underneath the TPS has to be beefed up.

The CS for the HS was 12 pcf H/C 2" thick with 0.80" thick face sheets.

The CS for the BS was 12 pcf H/C 1.5" thick with 0.050" thick face sheets.

The PICA thickness was not changed from VME to this case.

A thick aluminum mounting ring - 0.125 Solid Aluminum Plate Mounting Ring (estimated to be ~80 kg) required to attach the aeroshell to the internal payload was not considered as part of aeroshell but assumed to be accounted for in the mechanical system.

APPENDIX E – CONTEXT IMAGER

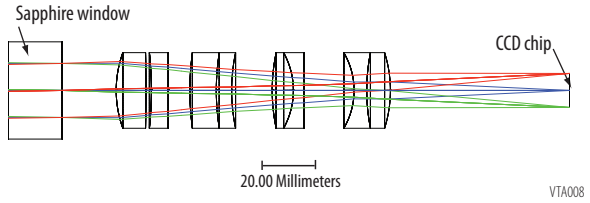


Figure E1: Figure Raman/LIBS context imager

APPENDIX F - ACRONYMS LIST

Acronym	Definition
ADL	Goddard Space Flight Center's Architecture Design Lab
ARC	Ames Research Center
ASI	Atmosphere Structure Investigation
B	billion
BPSK	Binary Phase Shift Keying
C	Celcius
C3	launch energy
CBE	Current Best Estimate
CCD	Charge Coupled Device
CD&H	Command and Data Handling
cg	center-of-gravity
cm	centimeter
CMCP	Chopped Molded Carbon Phenolic
CML	Concept Maturity Level
CO2	carbon dioxide
CP	Carbon Phenolic
D/H	Deuterium/Hydrogen
DLA	Declination of Launch Asymptote
DOD	Depth Of Discharge
DSN	Deep Space Network
EDE	Entry and Descent Element
EFPA	Entry Flight Path Angle
EM	Engineering Model
FOV	Field-Of-View
FWHM	Full Width at Half Maximum
FY	Fiscal Year
g	measurement versus earth gravitational acceleration (9.81 m/s^2)
GN&C	Guidance Navigation and Control
GSFC	Goddard Space Flight Center
HGA	High Gain Antenna
Hz	Hertz
I&T	I&T
K	Kelvin
Ka-band	Ka-band Communication frequencies of 26.5-40GHz
kbps	kilobits pers second
kg	kilogram
km/s	kilometers per second
kW	kilowatt
LNT	lithium nitrate trihydrate
m	meter
M	million
m/s	meters per second

Acronym	Definition
Mbits	Megabits
MEL	Master Equipment List
mJ	millijoules
MLI	Multi-Layer Insulation
mm	millimeter
MOSFETS	Metal–Oxide–Semiconductor Field-Effect Transistor
MSC/NASTRAN	MacNeal-Schwendler Corp (mechanical analysis software)
MSL	Mars Science Laboratory
NIR	Near Infrared
nm	nanometer
NMS	Neutral Mass Spectrometer
OSR	Optical Solar Reflectors
PCM	Phase Change Material
PICA	Phenolic Impregnated Carbon Ablator
PVLP	Pioneer Venus Large Probe
Raman/LIBS	Laser Induced Breakdown Spectroscopy
RF	Radio Frequency
RMS	Root Mean Square
S-band	2 to 4 GHz Communications Band
S/C	spacecraft
S/N	Signal-to-Noise
SAR	Synthetic Aperature Radar
SBC	Single Board Computer
SINDA	Systems Improved Numerical Differencing Analyzer
SRR	System Requirements Review
TLS	Tunable Laser Spectrometer
TPS	Thermal Protection System
TRL	Technology Readiness Level
TWCP	Tape Wrapped Carbon Phenolic
TWTA	Traveling Wave Tube Amplifier
V	Volt
IAU	International Astronomical Union (planetary coordinate system)
VEx	Venus Express
VEXAG	Venus EXploration Analysis Group
VITaL	Venus Intrepid Tessera Lander
VME	Venus Mobile Explorer
VOI	Venus Orbit Insertion
W	Watt
X-band	X-band is 7.0 to 11.2 gigahertz
XRD/XRFS	X-Ray Diffraction/X-Ray Fluorescence
µm	micrometer

APPENDIX G - REFERENCES

Arvidson R., R. Greeley, M. Malin, R. Saunders, N. Izenberg, J. Plaut, E. Stofan and M. Shepard (1992) Surface modification of Venus as inferred from Magellan observations of plains, *J. Geophys. Res.*, 97(E8) doi:10.1029/92JE0134.

Bindschadler, D.L., and Head, J.W., 1989, Characterization of Venera 15/16 geologic units from Pioneer Venus reflectivity and roughness data: *Icarus*, v. 77, p. 3-20.

Bullock, M. (2009) Venus Flagship Mission Study: Report of the Venus Science and Technology Definition Team.

Campbell, B. and Campbell, D. (1992) Analysis of volcanic surface morphology on Venus from comparisin of Arecibo, Magellan and terrestrial airborne radar data, *J. Geophys. Res.* 97(E10) doi:10.1029/92JE01558.

Clegg, S. M., Barefield, J. E., Wiens, R. C., Quick, C. R., Sharma, S. K., Misra, A. K., M. D. Dyar, M. D., McCanta, M. C., and Elkins-Tanton, L. (2009) Venus Geochemical Analysis by Remote Raman – Laser Induced Breakdown Spectroscopy (Raman-LIBS), *Venus Geochemistry: Progress, Prospects, and New Missions* (2009)

Connors C. and J. Suppe (2001) Constraints on magnitudes of extension on Venus from slope measurements. *J. Geophys. Res.*, 106 (E2) doi:10.1029/2000JE001256.

Crisp, D., JPL presentation, "The Solar and Thermal Radiation Field below The Venus Clouds", 2000

Florensky, C. P., L. B. Ronca, A. T. Basilevsky, G. A. Burba, O. V. Nikolaeva, A. A. Pronin, A> M. Trakhtman, V. P. Volkov and V. V. Zazetsky (1977) The surface of Venus as revealed by Soviet Venera 9 and 10, *Geol. Soc. Am. Bull.*, 88, 1537-1545.

Ford, P. G. and Pettengill, G. H. (1992) Venus topography and kilometer-scale slopes, J. Geophys. Res., 97, 13103-13114.

Hashimoto G. L., M. Roos-Serote, S. Sugita, M. S. Gilmore, L. W. Kamp, R. W. Carlson and K. H. Baines (2008) Felsic highland crust on Venus suggested by Galileo Near-Infrared Mapping Spectrometer data. *J. Geophys. Res.*, 113, doi:10.1029/2008JE003134.

Herrick R. R., D. L. Stahlke and V. L. Sharpton (2010) A new data set for Venus: Stereo-derived topography for 20% of the planet at km-scale horizontal resolution, Lunar Plan. Sci. Conf. 41, Abstract #1622.

Ivanov, M. A. (2009) Comparison of RMS slopes of terrestrial examples and tessera terrain, Venus, 50th Brown Vernadsky Microsymposium, Moscow, Russia.

Mueller N., J. Helbert, G. L. Hashimoto, C. C. C. Tsang, S. Erard, G. Piccolini and P. Drossart (2008) Venus surface thermal emission at 1 micron in VIRTIS imaging observations: Evidence for variation of crust and mantle differentiation conditions. *J. Geophys. Res.* 113, doi:10.1029/2008JE003118.

Sharma, S. K., A.K. Misra, P.G. Lucey, R.C. Wiens, S.M. Clegg (2007) Combined remote LIBS and Raman spectroscopy at 8.6m of sulfur-containing minerals, and minerals coated with hematite or covered with basaltic dust, *Spectrochimica Acta Part A 68* (2007) 1036–1045

Smrekar, S., S. Limaye, et al. (2009) Venus Exploration Analysis Group Goals, Objectives, Investigations and Priorities.

Wiens, R. C., Shiv K. Sharma, Justin Thompson, Anupam Misra, Paul G. Lucey (2005) Joint analyses by laser-induced breakdown spectroscopy (LIBS) and Raman spectroscopy at stand-off distances, *Spectrochimica Acta Part A 61* (2005) 2324–2334

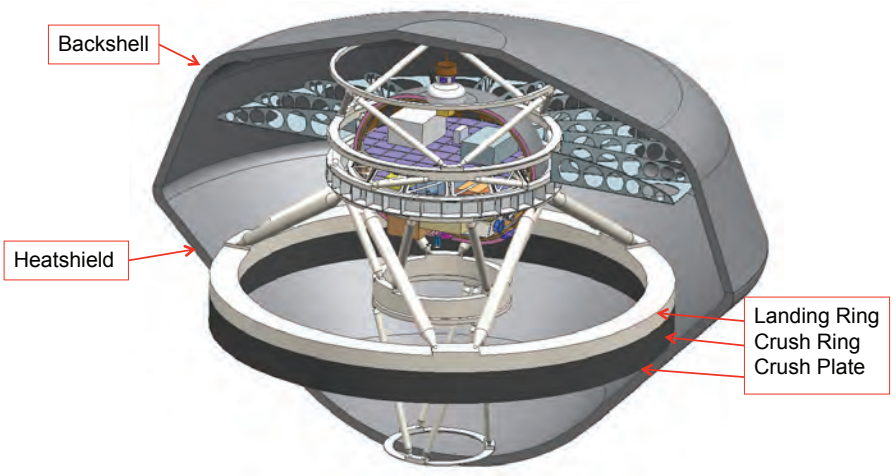
Appendix: ViTAL Aeroshell

Ames Contributing Members Team:
Gary Allen, Ken Hamm, Helen Hwang, Bernie Laub,
Jim Ross, Todd White, Ethiraj Venkatapathy

Date: 3/15/2010

3/31/10

Cross Section View of Heat shield and Back shell



2/10/2010 2

Aeroshell Mass Summary:

- Components:
 - Heat shield, Back Shell and Parachute
 - Heat shield: Carbon Phenolic bonded to a 2" Honeycomb (Al with Composite face-sheet)
 - Back shell: PICA tiles bonded to a 1.5" Honeycomb (Al with Composite face-sheet)
 - Parachute sized based on simple mass scaling (3 *(P-V large probe parachute) based on guidance from Pioneer Aerospace)
- Key Assumptions:
 - Ve = 11.3 km/s; EFPA = -23.35 deg; Max Dia: 3.5; P-V scaled

	Zero Margin	with 30% Margin
Aeroshell Mass	1050	1364.9667
Payload mass, kg	1200	1560
Total Entry Mass,	**2250**	**2925**

3/31/10

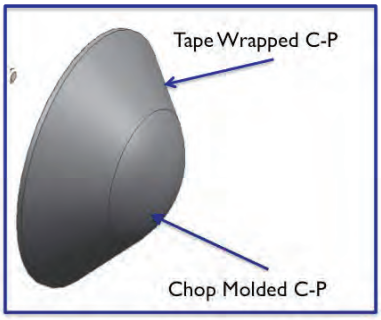
Detailed Mass Summary

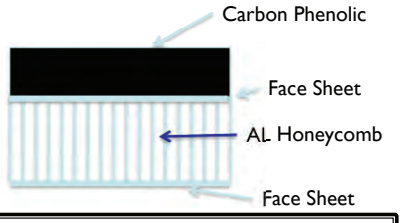
Aeroshell + Parachute	
	Zero Margin
Max Dia,m	3.5
BS Mass, kg	293
HS Mass, kg	717
Parachute, kg	40
Total, kg	1050

	Zero Margin
Max Dia,m	3.5
BS structure	224
BS TPS	69
BS Total Mass, kg	**293**
HS structures	269
HS TPS (C-P)	449
HS Total Mass, kg	**717**
Parachute, kg	**40**
Total, kg	**1050**

3/31/10

Heat Shield





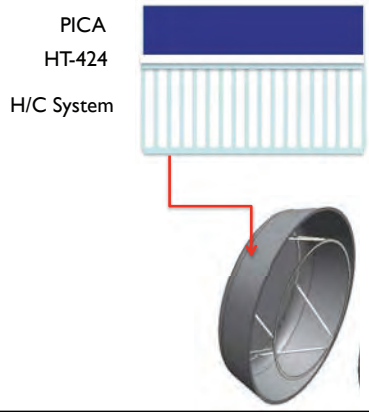
Avrg. Thickness of C-P:	2.325 cm"
Face Sheet:	0.08 in
Al H/C (12 lbs/ft^3) density at 2" thick	
Carbon Phenolic Mass:	**449 kg**
Carrier Structure Mass:	**269 kg**
HS Total Mass	**717 kg**

3/31/10

Back Shell

- Back shell TPS is PICA tiles bonded to the underlying carrier structure (Al H/C with composite face sheet.
- Approximately 100 PICA tiles (1.25 cm x 39.7 cm x 39.7 cm)
- The tiles are bonded to the CS with 20 mil HT-424 adhesive
- The tile gap between tiles are filled with RTV (80 mil gap)

PICA Thickness:	1.25 cm
HT-424:	20 mil
HC face sheet:	30 mil
HC:	1.5 inch
PICA Mass:	52.8 kg
HT 424 Mass:	12.9 kg
RTV Carrier Structure Mass:	223.9 kg
Total TPS mass (PICA+RTV+HT424)	68.93 kg
Total backshell structures mass	223.93 kg
Area of Backshell	15.79 m2
Areal Density of BS:	14.18 kg/m2
Total Back shell mass:	292.85 kg



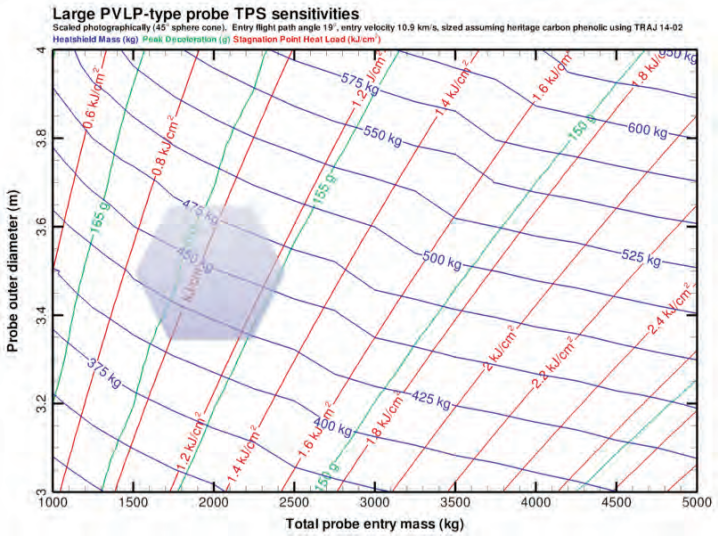
3/31/10

Individual Presentations that summarizes numerous studies:

- HS Mass Sensitivity Carpet plot
- BS PICA Thickness Sensitivity Carpet plot
- Max conditions (EFPA of -23.35 deg and ballistic coeff of 294 kg/m^2)
- ViTAL Aeroshell Structure
- Aero stability Assessment: Comments on Lander Configuration
- Preliminary Experimental Low-Speed Drag and Stability Measurements of Potential Probe Configurations (6/19/03)

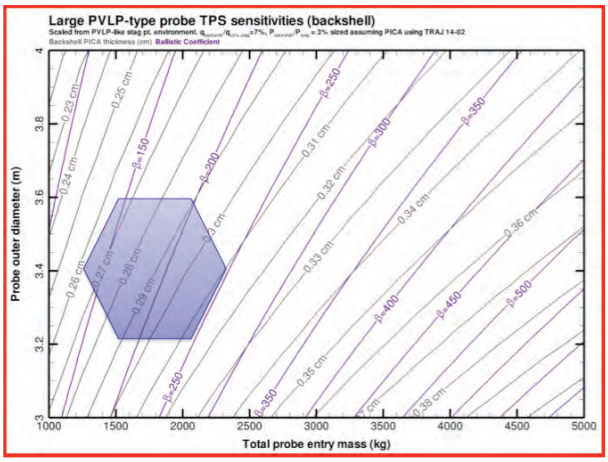
3/31/10

HS Mass Sensitivity Carpet plot



3/31/10

BS PICA Thickness Sensitivity Carpet plot



3/31/10

PICA thickness on the back shell is decided based on manufacturing and handling consideration: 1.25 cm (is >> PICA thickness needed based on engineering estimate of thermal load)

Raj Venkatapathy
G. Allen

ASSESSMENT: ENTRY VELOCITY impact on G' load

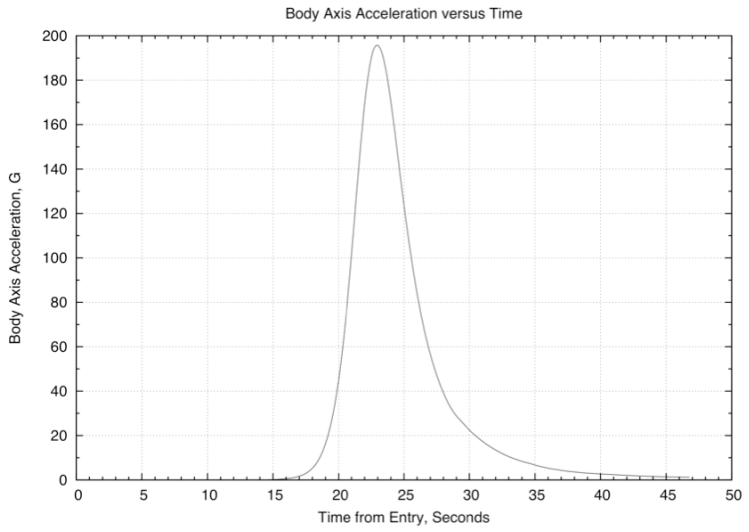
V_E = 11.3

3/31/10

Max Conditions including G'load during entry for Ve= 11.3 km/s and Ballistic Coefficient of 294 kg/m^2

Maximum Values					
Value	Quantity	Time (sec)	Altitude (km)	Velocity (km/sec)	Ball.Coef. (kg/m^2)
Deceleration Magnitude	1920.19 m/sec^2 195.80 G	23.0	76.90	7.13	294.19
Dyn. Pressure	5.65e+05 pascals	23.0	76.90	7.13	294.19
Stg. Pressure	1.10e+06 pascals	23.0	76.90	7.13	294.19
Cnv. Heat Flux	1445.93 W/cm^2	21.3	82.14	9.85	293.24
Rad. Heat Flux	3189.22 W/cm^2	20.8	84.23	10.42	293.57
Tot. Heat Flux	4571.50 W/cm^2	20.9	84.01	10.37	293.52
Wall Temp.	3500.00 K	Same as above line.			

G'load Profile during entry for Ve= 11.3 km/s and Ballistic Coefficient of 294 kg/m^2



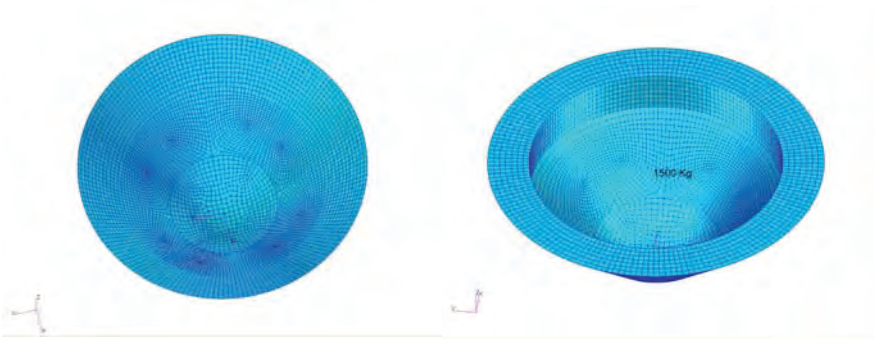
ViTAL Aeroshell Structure Sizing Iteration 2

February 3, 2010

Design Assumptions

- Geometry is similar to Pioneer Venus (45 degree sphere cone) scaled up to max diameter
 - 3.5 M
- Internal Payload of 1500 kg (3300 lbs)
- NSM for Carbon Phenolic HS 1" thick (ρ = 0.0534 pci)
- Deceleration load of 225 G.
 - Modeled as uniform pressure normal to Aeroshell surface
 - 3.5 M => 121.86 psi

Model Geometry

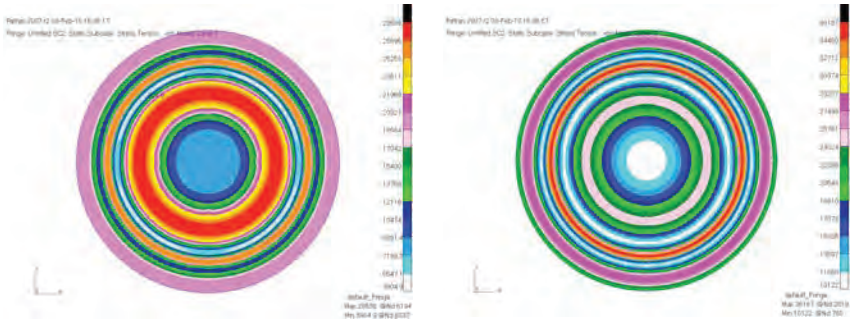


Outer Surface

Inner Surface

- Shell Elements used throughout
- Composite Modeling - .080” Aluminum Face sheets – 2.0” Al core (12 pcf)
- Inertia Relief Analysis used

Face Sheet Stress

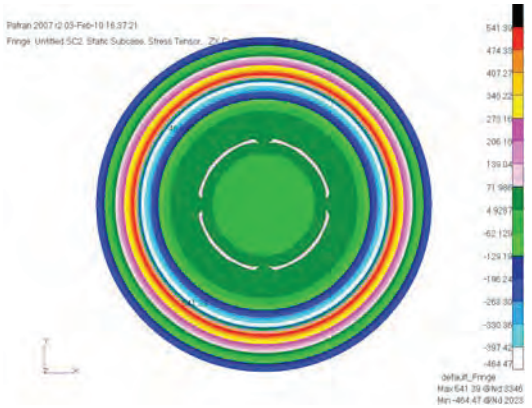


Outer Face Sheet
Max Von mises Stress = 29 ksi

Inner Face Sheet
Max Von mises Stress = 36 ksi

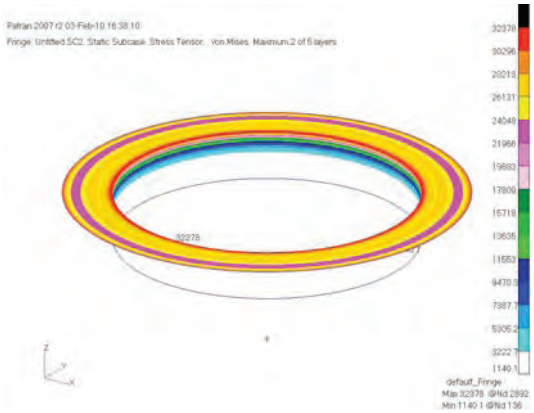
Assuming 2024-T3 Facesheets: Ftu = 64ksi, Fty = 47ksi, Fcy = 39ksi, Fsu = 39ksi
Min Margin (Compression Yield) = +0.08 (FoS 1.4, 1.0)

Core Shear



Max Shear = 542 psi
Shear Strength (min) = 1000 psi
Margin = +0.32 (FoS 1.4)

Mounting Ring



Max Von Mises = 32 ksi
Compression Yield = 39 ksi
Margin = +0.22 (FoS 1.4, 1.0)

Mass

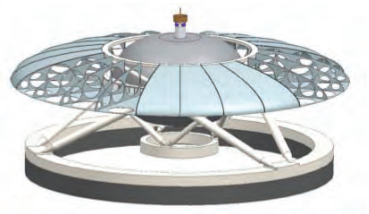
- Based on Stress Results seen for 3.5M Configuration
 - Configuration
 - 0.080” Face Sheets - Aluminum 2024-T3
 - 2.0” 1/8”-5052-.003 Aluminum Core (12pcf)
 - 0.125 Solid Aluminum Plate Mounting Ring
 - 3.5M Aeroshell Mass with the mounting ring = 768 lbs (349 kg)
 - Includes Mounting Ring
 - 1” Carbon Phenolic HS assumed = 1103 lbs NSM
 - The mounting ring is considered part of the mechanical system and hence not included in the Aeroshell Mass
 - Heat shiedl structural mass is: 269 kg
- More optimization needed
 - Contingency of 30% should be included on Mass Estimates
 - No Back Shell Mass Estimated
 - No Other Internal Structure Mass Estimated

Aero stability Assessment: Comments on Lander Configuration

Jim Ross
Code AOX
Feb 2010

Initial thoughts based on this image

- Good high-drag configuration
- High “aspect ratio” – short and wide – may lead to static and dynamic instability
 - Center of pressure is close to center of gravity
 - Wake from wide drag disk could couple with probe pitch motion leading to dynamic instability
- Landing ring wake can interact with the drag disk during pitch oscillation also leading to a static and/or dynamic instability
- The sharp corner on the drag disk is good but the circular shape may have periodic shedding – may be better to have several notches around the perimeter

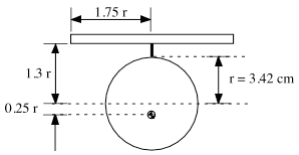


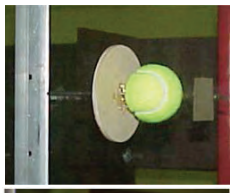
Preliminary Low-Speed Drag and Stability Measurements of Potential Probe Configurations 6/19/03

Jim Ross, et. al.

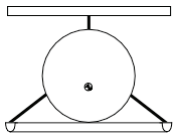
Configurations Tested

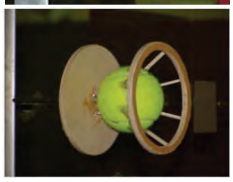
Case 1: Baseline



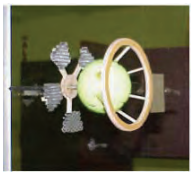


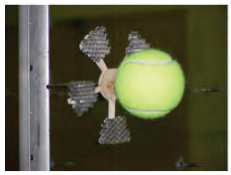
Case 2: With landing ring (scaled off Venera photo from web)





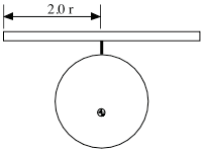
Cases 4 & 5: Fixed grid fins instead of drag plate - without (4) & with (5) landing ring





Configurations Tested, cont.

Cases 8 & 9: Sphere and Venera-size disk - without (8) and with (9) landing ring



For moment measurements, axis of torque sensor passed through the cg location indicated

$$C_D = \frac{D}{\pi r^2 q} \qquad C_M = \frac{M}{\pi r^3 q}$$

Moment measured at 0 & ±5°

Summary of Results

	C_D	$C_{M\alpha}$
• Case 1	3.40	-0.21
• Case 2	3.75	-0.21
• Case 4	1.19	-0.09
• Case 5	2.44	-0.06
• Case 8	5.72	-0.39
• Case 9	5.40	-0.38

These data were taken at Re ~200,000. At touchdown of 10 m/s, probe will be at Re~ 30,000,000 (based on r). Sphere model used has no Re dependence for drag but wake interactions between landing ring and sphere on disks and vanes could be different at high Re.

Comments

- Data are good for comparisons between configurations - not intended as absolute
- Landing ring has small, but measurable destabilizing influence at angles less than ±5° - data taken at 10 and 15° shows neutral stability for both the 1.75r and 2.0r drag disks
- Grid fins as tested produce low drag and low stability